

1-Fan-Bundle-Planar Drawings of Graphs

P. Angelini¹, M. A. Bekos¹, M. Kaufmann¹, P. Kindermann², and T. Schneck¹

¹*Institut für Informatik, Universität Tübingen, Germany,
{angelini,bekos,mk,schneck}@informatik.uni-tuebingen.de*

²*LG Theoretische Informatik, FernUniversität in Hagen, Germany,
philipp.kindermann@fernuni-hagen.de*

Abstract

Edge bundling is an important concept, heavily used for graph visualization purposes. To enable the comparison with other established nearly-planarity models in graph drawing, we formulate a new edge-bundling model which is inspired by the recently introduced fan-planar graphs. In particular, we restrict the bundling to the endsegments of the edges. Similarly to 1-planarity, we call our model *1-fan-bundle-planarity*, as we allow at most one crossing per bundle.

For the two variants where we allow either one or, more naturally, both endsegments of each edge to be part of bundles, we present edge density results and consider various recognition questions, not only for general graphs, but also for the outer and 2-layer variants. We conclude with a series of challenging questions.

1 Introduction

Edge bundling is a powerful tool used in information visualization to avoid visual clutter. In fact, when the edge density of the network is too high, the traditional techniques of graph layouts and flow maps become unusable. In this case, grouping together parts of edges that flow parallel to each other within a single bundle allows us to reduce the clutter and improve readability; see Fig. 1 for an example. Among the many, we mention here only the seminal papers of Holten [25] and Telea and Ersoy [35], which focus on radial layouts, as well as works on flow maps [11] and parallel coordinates [37]. For a comprehensive overview and an evaluation refer to Zhou et al. [36]. Confluent drawings [17] represent edges by planar curves that are not interior-disjoint, so the parts that are used by several edges can be interpreted as bundles, and in contrast to other edge bundling techniques, they are not ambiguous.

In this work, we combine the powerful visualization technique of edge bundling with previous theoretical considerations from the area of *beyond-planarity*, which is currently receiving strong attention (see, e.g., [12, 28, 29]). This area focuses on drawings of graphs in which in addition to a planar graph structure some crossings may be allowed, if they are limited to locally defined configurations. Different constraints on the crossing configurations define different *nearly-planar* graph classes. Classical examples are *1-planar* graphs [33], which allow for drawings in which each edge is crossed at most once, and *quasi-planar* graphs [1], which admit drawings not containing three mutually crossing edges.

Another typical example of nearly-planar graphs is the class of *fan-planar* graphs [30]. In a *fan-planar drawing* [6, 7, 8, 30], an edge is allowed to cross multiple edges as long as they belong to the same *fan*, that is, they are all incident to the same vertex; refer

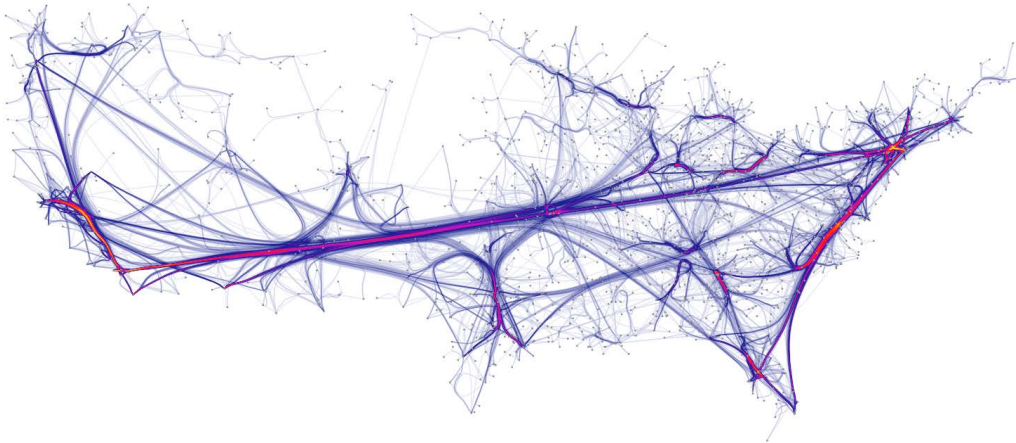


Figure 1: An example of edge bundling (taken from [26]).

to Fig. 2a. Such a crossing is called a *fan crossing*. The idea is that edges incident to the same vertex are somehow close to each other, and thus having an edge crossing all of them does not affect readability too much. In other words, edges of a fan can be grouped into a *bundle* such that the crossings between an edge and all the edges of the fan become a single crossing. In Fig. 2b we show the bundle-like edge routing corresponding to the fan-planar drawing in Fig. 2a. Note, however, that the original definition of fan-planar drawings does not always allow for this type of bundling, as in the case of graph $K_{4,n-4}$, for large enough n (see Section 4).

We thus introduce *1-fan-bundle-planar* drawings (*1-fbp* drawings for short), in which edges of a fan can be bundled together and crossings between bundles are allowed as long as each bundle is crossed by at most one other bundle; see Figs. 2b–2d. More formally, in a 1-fbp drawing every edge has 3 parts: the first and the last parts are *fan-bundles*, which may be shared by several edges, while the middle part is *unbundled*. Each fan-bundle can cross at most one other fan-bundle, while the unbundled parts are crossing-free. We remark that fan-bundles are not allowed to branch, that is, each fan-bundle has exactly two end points: one of them is the vertex the fan is incident to, while at the other one all the edges in the fan are separated from each other.

The latter “1-planarity” restriction prevents a fan-bundle of an edge to cross edges of several fans, which would be not allowed in a fan-planar drawing. However, since every edge has two fan-bundles, each of which can cross another bundle, it is still possible that an edge crosses two different fans, hence making the drawing not fan-planar. In order to avoid this, we introduce a restricted model of 1-fbp drawings, called *1-sided*, in which an edge can be bundled with other edges only on one of its two end vertices, that is, each edge has only one fan-bundle; see Figs. 2b and 2d. This restriction immediately implies

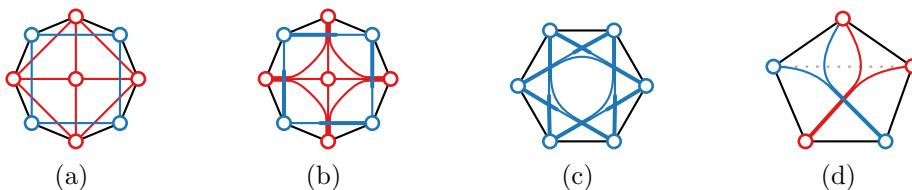


Figure 2: (a–b) The fan-planar graph of (a) is redrawn in (b) under the 1-sided model, (c) a 2-sided 1-fbp drawing of K_6 , (d) a 1-sided 1-fbp drawing of $K_5 \setminus e$ (the missing edge is drawn dotted).

Table 1: Lower bounds (LB) and upper bounds (UB) on the number of edges of 1- and 2-sided 1-fbp graphs.

Model	2-layer			outer			general		
	LB	UB	Th.	LB	UB	Th.	LB	UB	Th.
1-sided	$\frac{5n-7}{3}$	$\frac{5n-7}{3}$	7	$\frac{8n-13}{3}$	$\frac{8n-13}{3}$	6	$\frac{13n-26}{3}$	$\frac{13n-26}{3}$	5
2-sided	$2n - 4$	$3n - 7$	13	$4n - 9$	$4n - 9$	12	$6n - 18$	$\frac{43n-78}{5}$	15

that 1-sided 1-fbp drawings are fan-planar. Note that this is not the case for the model in which each edge has two fan-bundles, which we call *2-sided* (see Fig. 2c). In fact, we will prove in Section 4 that there exist 2-sided 1-fbp graphs that are not fan-planar, and vice versa.

Since each bundle collects a set of edges and allows them to participate in a crossing, natural beyond-planarity theoretical questions arise: (i) Characterize or recognize the graphs that admit (1- or 2-sided) 1-fbp drawings, and (ii) provide upper and lower bounds on their *edge density*, that is, the maximum number of edges they can have, expressed in terms of their number of vertices. More graph drawing related questions concern the use of this model embedded in commonly used approaches like hierarchical drawings [34], radial drawings [16], or force-directed methods [22].

We provide several answers to these questions under the 1-sided and the 2-sided models. We study these questions in the general case and in two restricted variants that have been commonly studied for other classes of nearly-planar graphs. Namely, in an *outer*-1-fbp drawing the vertices are incident to the unbounded face of the drawing, while in a *2-layer* 1-fbp drawing the graph is bipartite and the vertices of the two bipartition sets lie on two parallel lines, and the edges lie completely between these two lines.

Our Contribution. In Section 4, we study inclusion relationships between the classes of 1- and 2-sided 1-fbp graphs and other classes of nearly-planar graphs. Then, in Section 5, we present upper and lower bounds on the edge density of these classes; for an overview refer to Table 1. We then consider the complexity of the recognition problem; we prove in Section 6 that this problem is NP-complete in the general case for both the 1-sided and the 2-sided models, while in Section 7 we present linear-time recognition and drawing algorithms for biconnected 2-layer 1-fbp graphs, maximal 2-layer 1-fbp graphs, and triconnected outer-1-fbp graphs in the 1-sided model.

In Section 2 we present a short overview of the state of the art for beyond-planarity. Section 3 introduces preliminary notions and notation. We conclude in Section 8 by giving a list of open problems.

2 Related Work.

Over the last few years, several classes of nearly-planar graphs have been proposed and studied. Apart from *1-planar* [31, 33], *quasi-planar* [1], and *fan-planar* [30] graphs, which have already been discussed, other classes of nearly-planar graphs include: (i) *k-planar* [32], which generalize 1-planar graphs, as they admit drawings in which every edge is crossed at most k times; (ii) *fan-crossing free* [13], which complement fan-planar graphs, as they forbid fan crossings but allow each edge to cross any number of pairwise independent edges; (iii) *RAC* [18], which admit straight-line drawings where edges cross only at right angles; and (iv) the recently introduced *k-gap-planar* [5], which admit drawings where

each crossing is assigned to one of the two involved edges and each edge is assigned at most k of its crossings.

These classes have been mainly studied in terms of their edge density, and of the computational complexity of their corresponding recognition problem. From the density point of view, while the graphs in all these classes can be denser than planar graphs, all of them still have a linear number of edges [1, 5, 9, 13, 18, 30, 32]. From the recognition point of view, the problem has been proven to be NP-complete for most of the classes [2, 5, 8, 19], except for quasi-planar and fan-crossing free graphs, whose time complexities are still unknown. On the other hand, for the restricted outer and 2-layer cases, several polynomial-time algorithms have been proposed [3, 6, 14, 20, 15, 27].

Fink et al. [21] considered a different style of edge bundling, where groups of locally parallel edges are bundled and only bundled crossings are allowed.

3 Preliminaries

A graph G admitting a 1-sided (2-sided) 1-fbp drawing is called *1-sided* (*2-sided*, respectively) *1-fbp* graph. Graph G is *maximal* if the addition of any edge destroys its 1-fan-bundle-planarity, in any of its drawings. Analogously, we define the (maximal) 1-sided or 2-sided *outer-1-fbp* and *2-layer 1-fbp* graphs. The drawings we consider in this paper are *almost simple*, meaning that no two bundles of the same vertex cross. Note however that two edges incident to the same vertex might cross in the 2-sided model; see for an example Fig. 5f. A *rotation system* describes for each vertex an order of its incident edges as they appear around it.

A vertex u can be incident to more than one bundle. Let B_u be one such bundle. We say that B_u is *anchored at* vertex u , which is the *origin* of B_u . We denote by $|B_u|$ the *size* of B_u , that is, the number of edges represented by B_u . Clearly, $|B_u| \leq \deg(u)$. We refer to the endpoint of fan-bundle B_u different from u (where all the edges of B_u are separated from each other) as the *terminal* of B_u , and to the end vertex different from u of any edge in B_u as a *tip* of B_u . For two crossing fan-bundles B_u and B_v anchored at vertices u and v , we call *$B_u B_v$ -following curve* a curve that starts at u , follows B_u up to the crossing point with B_v , then follows B_v , and ends at v in such a way that it crosses neither bundles.

4 Relationships with other graph classes

In this section, we discuss inclusion relationships between the classes of 1-sided and 2-sided 1-fbp graphs and other relevant classes of nearly-planar graphs. In particular, we focus on the classes of 1-planar and fan-planar graphs, due to the immediate relationships determined by the definition of 1-fbp graphs. We also consider the well-studied class of 2-planar graphs [4], which has already been proven to be incomparable with the class of fan-planar graphs [8], despite the fact that their maximum edge-density is the same, namely $5n - 10$ [30, 32]. Our findings are summarized in Fig. 3.

The inclusion relationship $1\text{-PLANAR} \subseteq 1\text{-SIDED } 1\text{-FBP} \subseteq \text{FAN-PLANAR}$ follows from the definition of 1-sided 1-fbp graphs, and the same holds for the inclusion relationship $2\text{-PLANAR GRAPHS} \subseteq 2\text{-SIDED } 1\text{-FBP}$. Also, Binucci et al. [8] proved that the class of 2-planar graphs is incomparable with the class of fan-planar graphs. In particular, they showed that the 3-partite graph $K_{1,3,10}$ is fan-planar but not 2-planar and that the graph K_7^{13} , which is obtained by adjusting 13 copies of K_7 as depicted in Fig. 4, is 2-planar but not fan-planar.

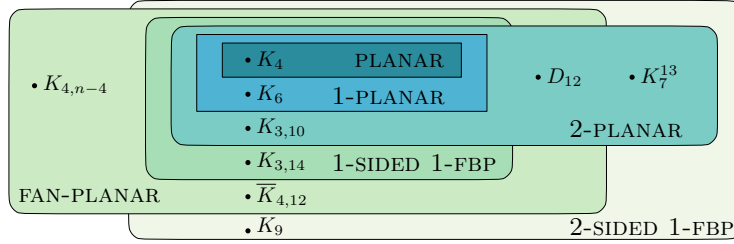


Figure 3: Relationships among graph classes proved in this paper. The graph denoted by $\overline{K}_{4,12}$ is obtained from the complete bipartite graph $K_{4,12}$ by joining the four vertices of its first bipartition set on a path and the twelve vertices of its second bipartition set on a second path (see Fig. 2(a) in [30] or Fig. 5d). The graph denoted by D_{12} corresponds to the graph obtained from the dodecahedral graph by adding a pentagram in each of its faces (see Fig. 2(b) in [30] or Fig. 5a). The graph denoted by K_7^{13} is obtained by appropriately adjusting 13 copies of K_7 (see Fig. 8 in [8] or Fig. 4).

We already know that K_4 is planar and that K_5 and K_6 are 1-planar, and hence belong to all classes that we consider here. Kaufmann and Ueckerdt [30] proved that the graph obtained from the dodecahedral graph by adding a pentagram in each of its faces (denoted by D_{12} in Fig. 3) is 2-planar, fan-planar, and meets exactly the maximum density of these classes of graphs, namely $5n - 10$; see Fig. 2(b) in [30] or Fig. 5a. As we will see in Section 5, this graph is too dense to be 1-sided 1-fbp (and hence 1-planar). Since K_9 contains more than $5n - 10$ edges, it is neither fan-planar nor 2-planar. On the other hand, K_9 is 2-sided 1-fbp, as shown in Fig. 5b. We do not know whether K_{10} is 2-sided 1-fbp or not, but we know that there exists some value of n for which K_n is not 2-sided 1-fbp, since 2-sided 1-fbp graphs have at most a linear number of edges, as we prove in Section 5. An interesting observation is that K_{10} admits a quasi-planar drawing [10].

In Fig. 5c, we show that the graph $\overline{K}_{4,12}$ obtained from the complete bipartite graph $K_{4,12}$ by joining the four vertices of its first bipartition set on a path and the twelve vertices of its second bipartition set on a second path is 2-sided 1-fbp. As shown in Fig. 5d, this graph is fan-planar [30], but not 2-planar (as it contains $K_{3,11}$ as a subgraph, which is not 2-planar; see Lemma 1). In addition, this particular graph cannot be 1-sided 1-fbp, as it contains 62 edges, while a 1-sided 1-fbp graph on 16 vertices cannot have more than 60 edges (see Section 5).

We now give a proof of our previous claim that $K_{3,11}$ is not 2-planar; note that even $K_{3,14}$ is 1-sided 1-fbp, as shown in Fig. 5e. We also show that $K_{3,10}$ is 2-planar, by means of a more general proof (which may be of its own interest) about the existence of k -planar drawings of graphs $K_{3,n-3}$ where n is a function of k . Note that in the proof of Lemma 1 we assume that edges incident to the same vertex are not allowed to cross, which is a

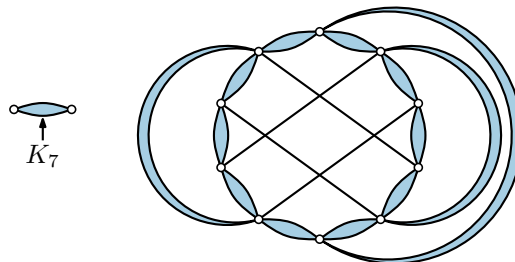


Figure 4: Illustration of the graph K_7^{13} which has the property that it is 2-planar, but not fan-planar [8].

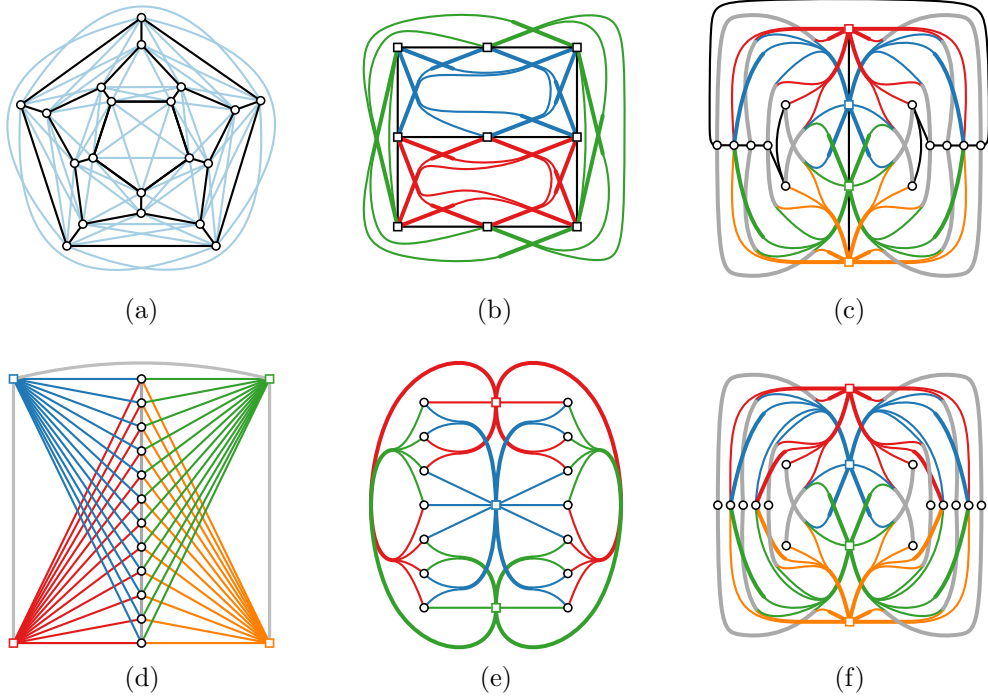


Figure 5: (a) A straight-line drawing of graph D_{12} obtained from the dodecahedral graph by adding a pentagram in each of its faces. (b) A 2-sided 1-fbp drawing of K_9 . (c) A 2-sided 1-fbp drawing of graph $\overline{K}_{4,12}$ obtained from the complete bipartite graph $K_{4,12}$ by joining on a path the four vertices of its first bipartition set and on a second path the 12 vertices of its second bipartition set. (d) A fan-planar drawing of $\overline{K}_{4,12}$. (e) A 1-sided 1-fbp drawing of $K_{3,14}$. (f) A 2-sided 1-fbp drawing of $K_{4,14}$.

reasonable assumption in the study of topological graphs, and consequently of k -planar graphs.

Lemma 1. *For each integer $k \geq 0$, graph $K_{3,4k+2}$ is k -planar, while graph $K_{3,4k+3}$ is not k -planar.*

Proof. For a complete bipartite graph $K_{3,n-3}$, let $U = \{u, v, w\}$ be the set of three vertices in the first bipartition set and let V be the set of $n - 3$ vertices in the second bipartition set. Also, let $E = U \times V$ be the set of its edges.

We show how to obtain a k -planar drawing of graph $K_{3,2k+1}$ such that the vertices in U are drawn on the horizontal line $y = 0$, the vertices in V are drawn on the horizontal line with $y = 1$, and each edge in E is drawn as a curve completely in the half plane above the horizontal line $y = 0$; see Fig. 6a.

Denote by $a_0, \dots, a_k, b_1, \dots, b_k$ the vertices of the second bipartition set of graph $K_{3,2k+1}$. We place vertex u at point $(-1, 0)$, vertex v at point $(0, 0)$, and vertex w at point $(1, 0)$. Then, for each $i = 0, \dots, k$, we place vertex a_i at point $(-\frac{i}{k}, 1)$. Symmetrically, for each $j = 1, \dots, k$, we place vertex b_j at point $(\frac{j}{k}, 1)$. We draw the edges of $K_{3,2k+1}$ as follows.

- E1. Each edge (v, a_i) , for $i = 0, \dots, k$ is drawn as a straight-line segment;
- E2. each edge (v, b_j) , for $j = 1, \dots, k$ is drawn as a straight-line segment;
- E3. each edge (u, a_i) , for $i = 0, \dots, k$, is drawn as a straight-line segment;

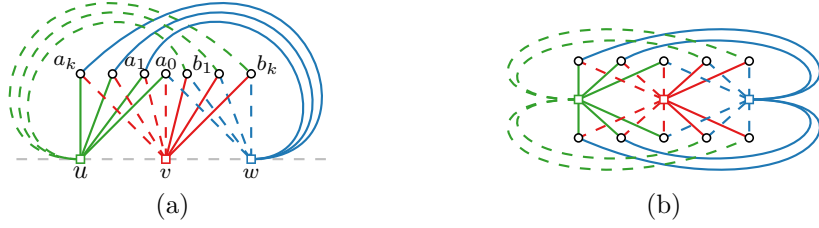


Figure 6: (a) A k -planar drawing of $K_{3,2k+1}$ in one half plane, and (b) a 2-planar drawing of $K_{3,10}$.

- E4. each edge (w, b_j) , for $j = 1, \dots, k$, is drawn as a straight-line segment;
- E5. edge (w, a_0) is drawn as a straight-line segment;
- E6. each edge (w, a_i) , for $i = 1, \dots, k$, is drawn as a curve that leaves a_i from the top, goes to the right around b_k , and enters w from the right, in such a way that $a_0, b_1, \dots, b_k, a_1, \dots, a_k$ appear in this clockwise order around w ;
- E7. each edge (u, b_j) , for $j = 1, \dots, k$, is drawn as a curve that leaves b_j from the top, goes to the left around a_k , and enters u from the left, in such a way that $a_0, a_1, \dots, a_k, b_1, \dots, b_k$ appear in this counterclockwise order around u .

That way, we will get the following crossings.

- C1. Edges (u, a_k) , (v, a_0) , and (w, b_k) are drawn crossing-free;
- C2. every edge (v, a_i) with $1 \leq i \leq k$ crosses exactly every edge (u, a_j) with $0 \leq j \leq i-1$, and thus it has at most k crossings;
- C3. every edge (u, a_j) with $1 \leq j \leq k-1$ crosses exactly every edge (v, a_i) with $j+1 \leq i \leq k$, and thus it has at most k crossings;
- C4. every edge (v, b_i) with $1 \leq i \leq k$ crosses exactly every edge (w, b_j) with $1 \leq j \leq i-1$, plus the edge (w, a_0) , and thus it has at most k crossings;
- C5. every edge (w, b_j) with $1 \leq j \leq k-1$ crosses exactly every edge (v, b_i) with $j+1 \leq i \leq k$, and thus it has at most k crossings;
- C6. edge (w, a_0) crosses every edge (v, b_j) with $1 \leq j \leq k$, and thus it has k crossings;
- C7. every edge (w, a_i) with $1 \leq i \leq k$ crosses exactly every edge (u, b_j) with $1 \leq j \leq k$, and thus it has k crossings;
- C8. every edge (u, b_j) with $1 \leq j \leq k$ crosses exactly every edge (w, a_i) with $1 \leq i \leq k$, and thus it has k crossings.

From the analysis above, it follows that no edge has more than k crossings. Hence, the constructed drawing of $K_{3,2k+1}$ is k -planar. To obtain a k -planar drawing for graph $K_{3,4k+2}$, we create two copies of the drawing of $K_{3,2k+1}$, mirror one of them at the horizontal line $y = 0$, and identify the vertices u, v, w in the two drawings. Fig. 6b shows such a 2-planar drawing for graph $K_{3,10}$. This completes the proof of the first part of the statement.

For the second part of the statement, assume to the contrary that for some $k \geq 0$ there is a k -planar drawing Γ of graph $G = K_{3,4k+3}$. As above, we denote by $U = \{u, v, w\}$ the first bipartition set of G and by $V = \{x_1, \dots, x_{4k+3}\}$ its second bipartition set.

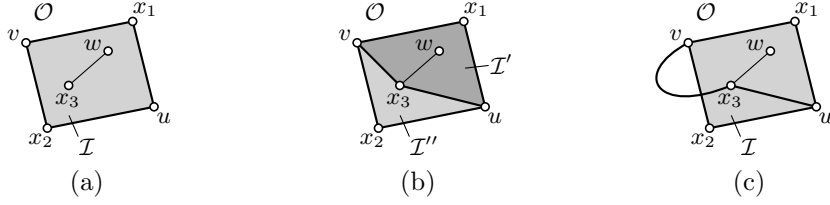


Figure 7: Illustration of the proof of Lemma 1: (a) w lies inside \mathcal{I} , (b) (u, x_3) and (v, x_3) are planar, and (c) (u, x_3) or (v, x_3) is crossed

We will first show that there is (at least) one subgraph $G' = K_{2,2}$ of G such that the drawing Γ' of G' contained in Γ is planar. For each $j = 2, \dots, 4k + 3$, let G_j be the subgraph of G induced by vertices u and v of the first bipartition set of G and by vertices x_1 and x_j of its second bipartition set. Note that all subgraphs G_2, \dots, G_{4k+3} have the edges (u, x_1) and (v, x_1) in common, which do not cross each other in Γ , because they are both incident to x_1 . Analogously, the edges (u, x_j) and (v, x_j) , with $2 \leq j \leq 4k + 3$, do not cross each other. Thus, in any subgraph G_j , we can only have a crossing between (u, x_1) and (v, x_j) , or between (v, x_1) and (u, x_j) . Since Γ is a k -planar drawing, the edges (u, x_1) and (v, x_1) can only be crossed $2k$ times in total. Hence, at least $2k + 2$ of the subgraphs from G_2, \dots, G_{4k+3} (i.e. excluding G_1) induce a crossing-free drawing.

Assume w.l.o.g. that the drawing Γ' of $G' = G_2$ contained in Γ is planar. Note that Γ' consists of a closed simple curve through u, x_1, v, x_2 ; see Fig. 7a. We denote by \mathcal{I} the bounded region enclosed by this curve, and by \mathcal{O} the unbounded region outside this curve. We will now show that w can lie neither in \mathcal{I} nor in \mathcal{O} .

Suppose that w lies in the bounded region \mathcal{I} . The case where w lies in the unbounded region \mathcal{O} is symmetric. Since G' has exactly four edges and Γ is a k -planar drawing, the edges of G' can be involved in at most $4k$ crossings in total. Since w is adjacent to all vertices x_3, \dots, x_{4k+3} , at least one of them, say x_3 , has to lie inside \mathcal{I} , as in Fig. 7a. If both edges (u, x_3) and (v, x_3) are drawn completely inside \mathcal{I} , then they split \mathcal{I} into two bounded regions \mathcal{I}' and \mathcal{I}'' , delimited by the closed curves through u, x_1, v, x_3 and through u, x_3, v, x_2 , respectively; see Fig. 7b. In this case, however, we could apply the same argument as above to say that there exists at least a vertex that lies in the interior of the same bounded region as w , either \mathcal{I}' or \mathcal{I}'' . Note that the bounded region we consider in this step is smaller and contains fewer vertices than \mathcal{I} . Thus, by repeating this argument at most a linear number of times, we can prove that there exists a vertex x_j , with $3 \leq j \leq 4k + 3$, lying inside the same bounded region \mathcal{I}^* as w , such that one of the edges (u, x_j) and (v, x_j) crosses an edge of the graph $G^* = K_{2,2}$ delimiting \mathcal{I}^* . To simplify the notation, assume $j = 3$, $G^* = G'$, and $\mathcal{I}^* = \mathcal{I}$; see Fig. 7c.

Hence, there are at most $4k - 1$ crossings between the edges of G' and edges not incident to x_3 . This implies that another one of the remaining $4k$ vertices x_4, \dots, x_{4k+3} must lie inside \mathcal{I} . By iteratively applying this argument, we conclude that all vertices x_3, \dots, x_{4k+3} have to lie inside \mathcal{I} and that, for every $i = 3, \dots, 4k + 3$, at least one of the edges (u, x_i) and (v, x_i) has to cross an edge of G' . However, this implies that the four edges of G' are involved in at least $4k + 1$ crossings in total; a contradiction. Thus, $K_{3,4k+3}$ has no k -planar drawing. \square

As already mentioned, the complete bipartite graph $K_{4,n-4}$ is fan-planar for every $n \geq 4$. In the following we will prove that there exists a value of n such that $K_{4,n-4}$ is not 2-sided 1-fbp, which also proves that fan-planar (and hence quasi-planar) graphs do not form

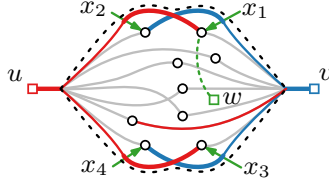


Figure 8: Illustration for the proof of Lemma 2, when there exist two intersecting pairs $\langle(u, x_1), (v, x_2)\rangle$ and $\langle(u, x_3), (v, x_4)\rangle$.

a subclass of 2-sided 1-fbp graphs. Note that a 2-sided 1-fbp drawing can be constructed for $K_{4,14}$; see Fig. 5f. Before we proceed with the detailed proof of our claim, we need two auxiliary lemmas.

Lemma 2. *Let Γ be a 2-sided 1-fbp drawing of graph $K_{3,9}$. Then, at least two of the vertices of the first bipartition set of $K_{3,9}$ must use more than one fan-bundle in Γ .*

Proof. Denote by $U = \{u, v, w\}$ the first bipartition set of $K_{3,9}$ and by $V = \{x_1, \dots, x_9\}$ its second bipartition set. Consider the graph $K_{2,9} = \{u, v\} \times V$ and assume that there exists a drawing Γ of this graph in which u and v are connected to all of x_1, \dots, x_9 by means of single fan-bundles B_u and B_v , respectively. In other words, there exists a fan-bundle B_u (a fan-bundle B_v) anchored at u (at v) whose tips are x_1, \dots, x_9 .

Consider two edges (u, x_i) and (v, x_j) , with $1 \leq i \neq j \leq 9$; if these edges cross each other in Γ , we say that they form an *intersecting pair*; see the two pairs $\langle(u, x_1), (v, x_2)\rangle$ and $\langle(u, x_3), (v, x_4)\rangle$ in Fig. 8. We show that, whatever is the number of intersecting pairs, it is not possible to add the third vertex w to Γ and connect it to all vertices x_1, \dots, x_9 , so to obtain a 2-sided 1-fbp drawing of $K_{3,9}$.

The proof is based on the following observation. For any two edges forming an intersecting pair $\langle(u, x_i), (v, x_j)\rangle$, consider the curve connecting the terminals of B_u and B_v , constructed as follows. First follow (u, x_i) from the terminal of B_u till the intersection point of the bundles anchored at x_i and x_j containing (u, x_i) and (v, x_j) , respectively; then follow (v, x_j) till the terminal of B_v ; see the black dotted lines in Fig. 8. By construction, this curve is not crossed by any edge in Γ that is not incident to either x_i or x_j . This already implies that there exist no three intersecting pairs. In this case, in fact, there exists no placement for w that allows us to connect it to all the vertices x_1, \dots, x_9 (and in particular to the at least six vertices among x_1, \dots, x_9 involved in the intersecting pairs) without crossing at least one of such curves.

Suppose now that there exist exactly two intersecting pairs, as in Fig 8. W.l.o.g., let $\langle(u, x_1), (v, x_2)\rangle$ and $\langle(u, x_3), (v, x_4)\rangle$ be these pairs. Since the two curves defined by these two pairs cannot be crossed in Γ , there exists one of the two regions, say R , delimited by these curves that contains all the vertices x_1, \dots, x_9 , as well as vertex w , in its interior.

Consider now the five vertices x_5, \dots, x_9 and the five paths between u and v passing through these vertices. Observe that the edges of these paths may cross each other, but the only crossings can be either between two edges incident to u or between two edges incident to v , as otherwise there would be an additional intersecting pair. Consider the subregions of R defined by the arrangement of the curves representing these paths. Note that these subregions are at least six, which happens when all the five paths are crossing-free. By the previous observation on the possible crossings between these paths, we can conclude that, if we place w in any of these subregions, either the edges connecting w to x_1 and x_2 , or those connecting w to x_3 and x_4 have to cross edges of at least three of the five paths; see Fig. 8. This is not possible, since the edges of two different paths cannot be bundled together and since any edge incident to w has only two fan-bundles.

The case in which there exists at most one intersecting pair is analogous. In fact, in this case we can consider the region R as the whole plane, and use the at least seven paths not involved in the intersecting pair to make the same argument as above. This concludes the proof of the lemma. \square

Lemma 3. *In any 2-sided 1-fbp drawing of graph $K_{3,n-3}$, there is a fan-bundle containing at least $(n-2)/8$ edge-segments.*

Proof. By Lemma 1, graph $K_{3,n-3}$ is not k -planar for $k \leq (n-6)/4$. This implies that in any drawing of $K_{3,n-3}$ there is at least one edge with at least $1 + (n-6)/4 = (n-2)/4$ crossings. Since in a 2-sided 1-fbp drawing every edge has crossings only at its two fan-bundles, there is one of such fan-bundles that crosses at least $(n-2)/8$ edges. Since all these edges must be bundled together, the statement follows. \square

We are now ready to give the detailed proof of our initial claim, i.e., that there exists a value of n such that $K_{4,n-4}$ is not 2-sided 1-fbp.

Theorem 4. *Graph $K_{4,n-4}$ is not 2-sided 1-fbp for $n \geq 571$.*

Proof. Assume to the contrary that $K_{4,n-4}$ admits a 2-sided 1-fbp drawing Γ for some $n \geq 571$. First, consider any subgraph $K_{3,n-4}$ of $K_{4,n-4}$. By Lemma 3, there exists a fan-bundle B_u anchored at a vertex u with at least $(n-3)/8$ edge-segments. Since all the vertices in the second bipartition set have degree 3, vertex u belongs to the first bipartition set. Consider now the subgraph $K_{3,(n-3)/8}$ of $K_{4,n-4}$ that is composed of the three vertices of the first bipartition set different from u and from the $(n-3)/8$ vertices that are connected to u by means of B_u . By Lemma 3, there exists a fan-bundle B_v anchored at a vertex v with at least $\frac{1+(n-3)/8}{8} = (n+5)/64$ edge-segments. Again, vertex v belongs to the first bipartition set.

We have now found $(n+5)/64$ vertices that are connected to u and to v by means of single fan-bundles B_u and B_v in Γ . For $n \geq 571$, this value is at least 9, which contradicts Lemma 2. Hence, the proof of the theorem follows. \square

5 Density

In the following section, we consider Turán-type problems for 1-fbp graphs. Namely, we ask what is the maximum number of edges that an n -vertex 1-sided or 2-sided 1-fbp graph can have. We provide answers to this question both in the general case of the problem and in the outer and 2-layer variants.

5.1 Density of 1-sided 1-fan-bundle-planar graphs

We first study the density of general 1-sided 1-fbp graphs, and then we appropriately adjust for the outer and 2-layer variants.

Theorem 5. *A 1-sided 1-fbp graph with $n \geq 3$ vertices has at most $(13n-26)/3$ edges, which is a tight bound for infinitely many values of n .*

Proof. Let Γ be a 1-sided 1-fbp drawing of a *maximally dense* 1-sided 1-fbp graph G with n vertices, namely, a graph of this class with the largest possible number of edges. To estimate the maximum number of edges that G may contain, we will first appropriately transform G into a (not necessarily simple) maximal planar graph that contains no pairs of *homotopic parallel edges*, i.e., both the interior and the exterior regions defined by any

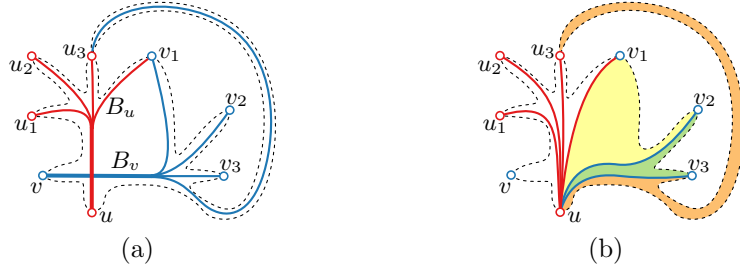


Figure 9: Illustration of the transformation used in the proof of Theorem 5 for the case $\mu = \nu = 4$. (a) Two crossing fan-bundles; observe that $v_1 = u_4$ and $u_3 = v_4$. (b) Our transformation which leads to two non-homotopic copies of (u, u_3) .

pair of parallel edges contain at least one vertex of G . Note that under this assumption, the maximum number of edges of a planar multi-graph with n vertices is still $3n - 6$. Since G is a drawn graph, we say that Γ *contains* an edge e if there exists a drawn edge of G in Γ that is homotopic to e .

Consider two crossing fan-bundles B_u and B_v in Γ anchored at vertices u and v of G , respectively; see Fig. 9a. Let $(u, u_1), \dots, (u, u_\mu)$ and $(v, v_1), \dots, (v, v_\nu)$ be the edges that are bundled in B_u and B_v , respectively, in the order in which they appear around the terminals of B_u and B_v in Γ , such that (u, u_1) and (v, v_1) are the edges that follow B_u and B_v along their terminals in clockwise direction. Note that the tips of fan-bundle B_u are not necessarily distinct from the tips of fan-bundle B_v , that is, for some pairs of indices i and j with $1 \leq i \leq \mu$ and $1 \leq j \leq \nu$ it may hold that $u_i = v_j$ (e.g., in Fig. 9a the third tip of B_u is identified with the fourth tip of B_v , or in other words $u_3 = v_4$). In particular, $v_1 = u_\mu$ holds by the maximality of G .

Consider the edge (u, v) that one can draw in Γ as a $B_u B_v$ -following curve. We refer to this particular edge as the *base-edge* of B_u and B_v . Since G is maximally dense, graph G must contain this edge, as otherwise one could add it in Γ without violating its 1-sided 1-fan-bundle-planarity or its non-homotopy. Similarly, one can prove that Γ contains edges $(v, u_1), (u_1, u_2), \dots, (u_{\mu-1}, u_\mu), (u_\mu, v_1), (v_1, v_2), \dots, (v_{\nu-1}, v_\nu)$, and (v_ν, u) that are drawn very close either to B_u and B_v or to the unbundled parts of the edges incident to u and v (refer to the dotted drawn edges of Fig. 9a).

We proceed by applying a simple transformation; see Fig. 9b. We remove from G all edges bundled in B_v and we introduce edges $(u, v_2), \dots, (u, v_{\nu-1})$ drawn without crossings in the interior of the region defined by edges $(u, v_1), (v_1, v_2), \dots, (v_{\nu-1}, v_\nu)$, and (v_ν, u) in Γ . Observe that this simple transformation does not introduce homotopic parallel edges and simultaneously eliminates the crossing between B_u and B_v . However, since Γ contains edges (v, v_1) and (v, v_ν) , which are not contained in the transformed drawing, our transformation leads to a reduction by at most two edges. In particular, it is not difficult to see that (C.1) if $\nu \neq 1$ and $\mu \neq 1$, then our transformation leads to a reduction by exactly two edges; (C.2) otherwise, it leads to a reduction by one edge.

By applying this transformation recursively to every pair of crossing fan-bundles, we will obtain a planar drawing Γ' of a (not necessarily simple) graph G' on the same set of vertices as G that contains no pairs of homotopic parallel edges. Hence, graph G' has at most $3n - 6$ edges and at most $2n - 4$ faces. Note that since the edges that are affected by a transformation are delimited by uncrossed edges, it follows that they will not be “destroyed” by another transformation later in our recursive procedure.

Now, observe that each transformation of Case C.1 produces at least three faces in

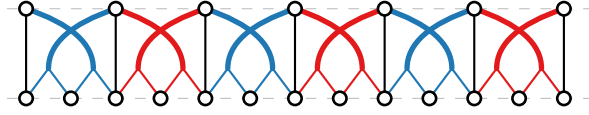


Figure 10: Illustration for the proof of Theorem 7.

G' and leads to a reduction by exactly two edges (see the colored faces of Fig. 9b). On the other hand, each transformation of Case C.2 produces two faces in G' and as already mentioned leads to a reduction by exactly one edge. Hence, graph G contains as many edges as G' plus twice the number of transformation of Case C.1, plus the number of transformations of Case C.2. Let f' and f'' be the number of faces of Γ' created by transformations of Case C.1 and C.2, respectively. It follows that $f' + f'' \leq 2n - 4$. Thus, G has at most $3n - 6 + 2 \cdot \lfloor f'/3 \rfloor + f''/2 \leq 3n - 6 + 2 \cdot \lfloor (2n - 4)/3 \rfloor \leq (13n - 26)/3$ edges.

To show that this upper bound is tight, consider a planar graph \mathcal{P}_n on n vertices whose faces are all of length 5. Hence, n must be appropriately chosen. By Euler's formula, graph \mathcal{P}_n has exactly $(5n - 10)/3$ edges and $(2n - 4)/3$ faces. In each face, it is possible to add four edges without violating 1-fan-bundle-planarity (see, e.g., Fig. 2d); thus, the resulting graph has $(5n - 10)/3 + 4 \cdot (2n - 4)/3 = (13n - 26)/3$ edges in total, and the statement follows. \square

The next two theorems present tight bounds for the density of 1-sided 1-fbp graphs in the outer and in the 2-layer models. The proofs are based on the same technique used in the proof of Theorem 5.

Theorem 6. *A 1-sided outer-1-fbp graph with $n \geq 5$ vertices has at most $(8n - 13)/3$ edges, which is a tight bound for infinitely many values of n .*

Proof. Let Γ be a 1-sided outer-1-fbp drawing of a maximally dense 1-sided outer-1-fbp graph G with n vertices. We apply the same transformation that we applied in the proof of Theorem 5. In this case, the resulting drawing Γ' is the drawing of an outerplanar graph G' on the same set of vertices as G . Hence, graph G' has at most $2n - 3$ edges and $n - 2$ internal faces. Using the same sequence of arguments as in the proof of Theorem 5, it follows that G has at most $2n - 3 + 2 \cdot \lfloor (n - 2)/3 \rfloor \leq (8n - 13)/3$ edges.

To show that this bound is tight, consider an outerplanar graph \mathcal{O}_n on n vertices whose internal faces are all of length 5. By Euler's formula, graph \mathcal{O}_n has $(4n - 5)/3$ edges and $(n - 2)/3$ internal faces. Since in each internal face of \mathcal{O}_n it is possible to add four edges without violating outer-1-fan-bundle-planarity (see, e.g., Fig. 2d), the resulting graph has $(4n - 5)/3 + 4 \cdot (n - 2)/3 = (8n - 13)/3$ edges in total, and the statement follows. \square

Theorem 7. *A 1-sided 2-layer 1-fbp graph with $n \geq 5$ vertices has at most $(5n - 7)/3$ edges, which is a tight bound for infinitely many values of n .*

Proof. Let G be a 1-sided 2-layer 1-fbp graph with n vertices. One can add $n - 2$ edges in G to connect in two paths the vertices of each bipartition set and obtain a new graph G' that is 1-sided outer-1-fbp. Since by Theorem 6 graph G' cannot have more than $(8n - 13)/3$ edges, it follows that G cannot have more than $(8n - 13)/3 - (n - 2) = (5n - 7)/3$ edges.

A graph \mathcal{B}_n with n vertices meeting exactly this bound can be easily constructed as follows. Let $n = 3k + 2$ for some positive integer k . Graph \mathcal{B}_n has $k + 1$ vertices in its first bipartition set and $2k + 1$ vertices in its second bipartition set. For each $j = 1, 2, \dots, k$ the vertices of the first bipartition set of \mathcal{B}_n with indices j and $(j + 1)$ form a $K_{2,3}$ with the vertices of the second bipartition set of \mathcal{B}_n with indices $(2j - 1)$, $2j$ and $(2j + 1)$; see

Fig. 10. Graph \mathcal{B}_n is indeed 1-sided 2-layer 1-fbp, as it consists of k consecutive copies of $K_{2,3}$ (which is a 1-sided 2-layer 1-fbp graph). To see that \mathcal{B}_n meets the density bound of this theorem observe that each of the k copies of $K_{2,3}$ contributes 6 edges in graph \mathcal{B}_n and that consecutive copies of $K_{2,3}$ share an edge. Hence, graph \mathcal{B}_n has $6k - (k - 1) = 5k + 1$ edges in total, and the statement follows. \square

5.2 Density of 2-sided 1-fan-bundle-planar graphs

As opposed to 1-sided 1-fbp graphs, 2-sided 1-fbp graphs are not necessarily fan-planar. In fact, they can be significantly denser than fan-planar graphs, as we will see later in this section. In the following, we will first present a tight bound on the density of 2-sided outer-1-fbp graphs. We then establish upper and lower bounds for the density of 2-sided 2-layer and 2-sided general 1-fbp graphs.

We start by presenting a family of 2-sided outer-1-fbp graphs with n vertices and $4n - 9$ edges. Before doing so, we introduce two definitions. A *flower drawing* of a graph with vertex-set $\{v_1, \dots, v_n\}$ is a 2-sided outer-1-fbp drawing in which (i) the vertices v_1, \dots, v_n lie on a circle \mathcal{C} in this clockwise order, (ii) each vertex v_i has two fan-bundles, a *right* and a *left* one; the right (left) fan-bundle is the one that is encountered first (second) when moving clockwise around v_i , starting from the outer face (in other words, when seen from the center of \mathcal{C} the left fan-bundle is to the left of the right fan-bundle), and (iii) for each $i = 1, \dots, n$, the right fan-bundle of v_i crosses the left fan-bundle of v_{i+1} (we assume the indices to be mod n); see Fig. 11a.

A *water lily* is a flower drawing of a graph with $n \geq 9$ vertices where the terminals of the fan-bundles are partitioned into three sets S_1 , S_2 , and S_3 , such that (i) each set S_j , for $j = 1, 2, 3$, contains at least seven consecutive terminals (e.g., the terminals contained in S_1 in Fig. 11a are the ones spanned by the orange arc), (ii) each pair of sets S_j and S_k , with $j \neq k$, have one terminal in common (refer to the terminals that are pointed by the arrows of the arcs indicating S_1 , S_2 and S_3 in Fig. 11a), which belongs to the right fan-bundle of a vertex, (iii) the terminal of the right fan-bundle of each vertex v_i is connected to the terminal of the left fan-bundles of vertices v_{i+1} and v_{i+2} , and (iv) the terminals in each set S_j , for $j = 1, 2, 3$, are connected by a *zigzag-pattern* such that all but two faces have degree 3, the other two have degree 4 in order to avoid parallel edges; see Fig. 11a.

Lemma 8. *There exist 2-sided outer-1-fbp graphs with n vertices and exactly $4n - 9$ edges, where $n \geq 9$.*

Proof. We prove the statement by showing that in a water lily on $n \geq 9$ vertices there exist $4n - 9$ edges. Namely, consider the graph H whose vertices are the terminals of the fan-bundles and whose edges are the unbundled parts of the edges of the water lily (drawn plain in Fig. 11a). First, observe that H has $2n$ vertices, since each original vertex has one left and one right fan-bundle. Also, H is biconnected and outerplanar, by the construction of the water lily. Finally, all the internal faces of H are triangular, except for six faces (two for each set S_j), each of which has degree 4. Since a biconnected outerplanar graph on ν vertices in which every internal faces is triangular has $2\nu - 3$ edges, we have that H has $2 \cdot (2n) - 3 - 6 = 4n - 9$ edges, and the statement follows. \square

Before we proceed with the proof of our upper bound on the edge density of 2-sided outer-1-fbp graphs, we first make a useful observation. If the vertices of the graph do not necessarily have to lie on the outer face of the drawing, one can draw another set of $2n - 9$ edges on the outer face of a water lily and obtain a 2-sided 1-fbp drawing of a graph

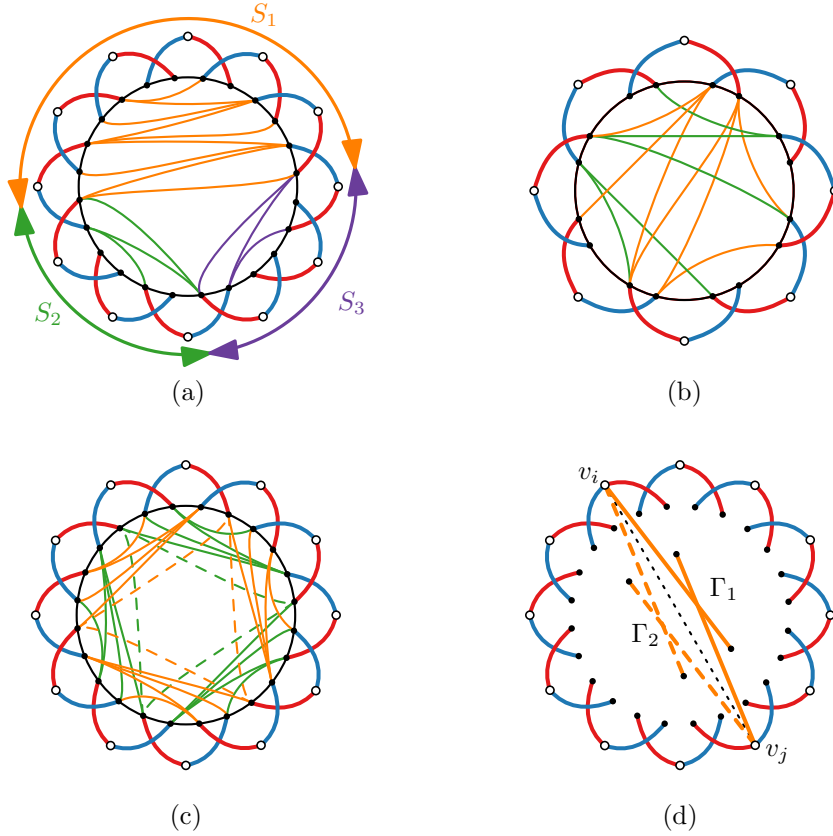


Figure 11: Illustration of: (a) a water lily, (b) a 2-sided 1-fbp drawing of K_8 , (c) a 2-sided 1-fbp drawing of a graph with n vertices and $6n - 18$ edges for $n = 12$, and (d) crossing middle fan-bundles. In (b) and (c) the orange edges can be drawn on the outer face of the drawing by using twice as many fan-bundles.

with $6n - 18$ edges. Note that this construction corresponds to merging two copies of a water lily on vertices v_1, \dots, v_n by identifying their vertices and by keeping only one copy of each edge (v_i, v_{i+1}) and (v_i, v_{i+2}) . With a little effort we can avoid potential parallel edges that may appear when merging the two copies. Let S_1, S_2, S_3 and S'_1, S'_2, S'_3 be the partitions of the terminals of the two copies. We require that the terminal shared by S'_j and S'_{j+1} belongs to S_j , for each $j = 1, 2, 3$ (where the indices are mod 3); see Fig. 11c. In this way, the zigzag patterns on S_1, S_2, S_3 and S'_1, S'_2, S'_3 are edge-disjoint, as desired. We summarize this observation in the following lemma.

Lemma 9. *There exist 2-sided 1-fbp graphs with n vertices and exactly $6n - 18$ edges, where $n \geq 9$.*

In the following theorem, we show that a 2-sided outer-1-fbp graph with n vertices cannot have more edges than a corresponding water lily with n vertices. This immediately implies that the bound of $4n - 9$ is tight for the edge density of 2-sided outer-1-fbp graphs.

Consider a 2-sided outer-1-fbp graph G together with a corresponding drawing Γ . Let v_1, \dots, v_n be the vertices of G as they appear in clockwise order along the outer face of Γ . A vertex of G may be incident to several fan-bundles in Γ . We denote by $B_i^1 \dots B_i^\lambda$ the fan-bundles anchored at a vertex v_i , as they appear in clockwise order around v_i starting from the outer face. We call B_i^1 and B_i^λ the *right fan-bundle* and the *left fan-bundle* of v_i , respectively; we refer to the remaining fan-bundles anchored at v_i as *middle fan-bundles*.

We assume w.l.o.g. that the right fan-bundle of v_i crosses the left fan-bundle of v_{i+1} , and that the edge (v_i, v_{i+1}) is represented with a crossing-free unbundled part connecting their terminals. Note that indeed this is an assumption w.l.o.g. as v_i and v_{i+1} are consecutive along the outer face, and hence representing the edge (v_i, v_{i+1}) in this way does not forbid the presence of any other edge.

For our proof we will need two auxiliary lemmas, which consider a special case. Namely, every vertex of G has degree at least 5 and it has at most one middle fan-bundle; also if a vertex has a middle fan-bundle, then it is not involved in any crossing.

As in the proof of Lemma 8, consider the graph H whose vertices are the terminals of all the left, middle, and right fan-bundles in Γ and whose edges are the unbundled parts of the edges between such terminals. If we denote by k the number of vertices of G that have a middle fan-bundle, then H has $2n + k$ vertices. Since H is clearly outerplanar, it has at most $4n + 2k - 3$ edges. We refer to the edges that connect consecutive terminals along the outerface of H as *outer edges*. The remaining edges of H are referred to as *inner edges*.

Lemma 10. *Graph H has at most $2n - k$ outer edges.*

Proof. Since H is outerplanar on $2n + k$ vertices, it cannot have more than $2n + k$ outer edges. Consider now a vertex v_i of G with a middle fan-bundle in Γ . Then, the vertex of H corresponding to the terminal of the right fan-bundle of v_{i-1} lies between the vertices of H corresponding to the terminals of the left and of the middle fan-bundles of v_i along the outer face of H , which implies that there exist two outer edges of H that represent the same edge (v_i, v_{i-1}) of G . Since G is simple, only one of these outer edges can belong to H . For the same reason, there exist two outer edges of H that represent the same edge (v_i, v_{i+1}) of G . Since there exist in total k vertices with a middle fan-bundle, the lemma follows. \square

In the following lemma, we give also an upper bound on the number of inner edges of H . We do so assuming that all the $2n + k$ outer edges of H are present (i.e., even the ones that correspond to parallel edges in G); in other words, if an edge of G can be represented both as an outer and as an inner edge of H , then we choose the former option. Note that this assumption is without loss of generality, as it does not increase the number of inner edges of H .

Lemma 11. *Graph H has at most $2n + k - 9$ inner edges, assuming that all the $2n + k$ outer edges of H are present.*

Proof. Since H is outerplanar, it follows that H cannot have more than $2n + k - 3$ inner edges. Let \mathcal{T} be the *weak dual* of H , i.e., the graph whose vertices are the internal faces of H and whose edges connect pairs of faces sharing an edge in H .

Since H is biconnected outerplanar, graph \mathcal{T} is a tree, and thus it has at least two leaves. Let f be a leaf of \mathcal{T} and let $e = (x, y)$ be the unique inner edge incident to f . Assume w.l.o.g. that x is a terminal of a fan-bundle of vertex v_i of G , while y is a terminal of a fan-bundle of a vertex of G that follows vertex v_i in the clockwise order of the vertices of G along its outer face.

The first observation is that x and y cannot be at distance 2 along the outer face of H . For a proof by contradiction, assume that x and y are at distance 2 along the outer face of H . We distinguish the following three cases:

- C.1 Vertex x is the terminal of the left fan-bundle of vertex v_i of G . In this case, we distinguish two subcases; vertex v_i has a middle fan-bundle or not (see Figs. 12a

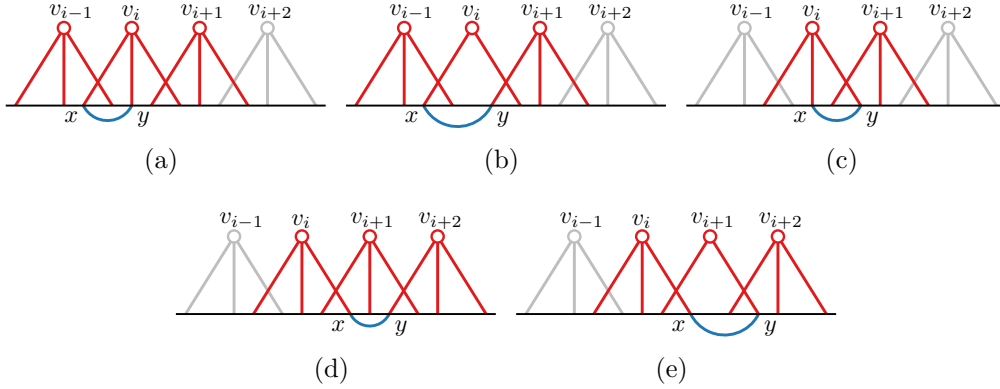


Figure 12: The five possible cases in which x and y are at distance 2 along the outer face of H .

and 12b, respectively). In the former case, edge (x, y) represents a self-loop in G , while in the latter case, edge (x, y) is already represented by an outer edge of H (in particular, by the outer edge of H that corresponds to the connection of the right fan-bundle of v_i with the left fan-bundle of v_{i+1}).

C.2 Vertex x is the terminal of the middle fan-bundle of vertex v_i of G . Since x and y are at distance 2, it follows that y is the terminal of the right fan-bundle of vertex v_i of G ; see Fig. 12c. This directly implies that (x, y) represents a self-loop in G .

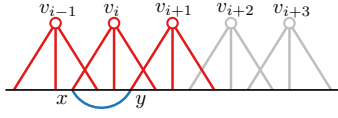
C.3 Vertex x is the terminal of the right fan-bundle of vertex v_i of G . In this case, we distinguish two subcases; vertex v_{i+1} has a middle fan-bundle or not (see Figs. 12d and 12e, respectively). In the former case, the middle fan-bundle of v_{i+1} does not contain an edge of G and therefore is redundant, while in the latter case, edge (x, y) is already represented by an outer edge of H .

From the above case analysis, it follows that x and y cannot be at distance 2 along the outer face of H , which implies that f cannot be a triangular face.

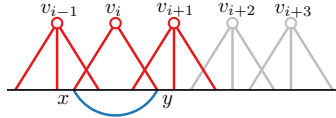
Consider now the cases in which x and y are at distance 3 or 4 along the outer face of H ; see Fig. 13. With a case analysis similar to the one above, we prove that the case in which edge e connects the right fan-bundle of v_i with the left fan-bundle of v_{i+3} , is the only case in which edge e (i) does not represent a self-loop of G , or (ii) does not represent an edge of G that is already represented by any outer edge of H , or (iii) does not yield a redundant middle fan-bundle; see Fig. 13g. Note that in this case the distance between x and y is indeed 3, and none of v_{i+1} and v_{i+2} has a middle fan-bundle.

We now claim that x and y cannot be at distance 5 (or more). In Fig. 14, we illustrate all cases that can appear when the distance between x and y is exactly 5. In all cases but one, either a middle fan-bundle is redundant or a vertex of G has degree less than 5, both of which form a contradiction (note that this also holds when x and y are at distance greater than 5). The exceptional case is illustrated in Fig. 14d. In this particular case, if x and y are at distance 5, then the contradiction is based on the fact that the edge (x, y) is represented as outer edge in H . On the other hand, if x and y are at distance greater than 5, then v_{i+1} has degree less than 5, which is again a contradiction. Hence, our claim follows. We can therefore assume that x and y are at distance 3, as in Fig. 13.

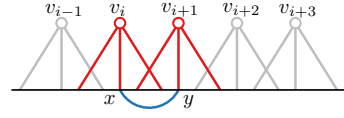
Let f' be the face that is incident to e and different from f . We prove that f' cannot be of degree 2 in \mathcal{T} . Suppose for a contradiction that f' has degree 2 in \mathcal{T} . Hence, there is only one inner edge $e' = (x', y')$ of H incident to f' that is different from e . Since x



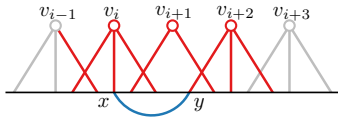
(a) Edge (x, y) is represented as outer edge.



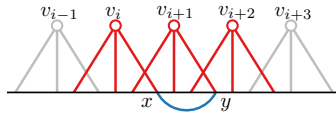
(b) Edge (x, y) represents a self-loop of G .



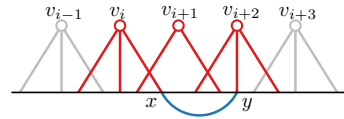
(c) Edge (x, y) is represented as outer edge.



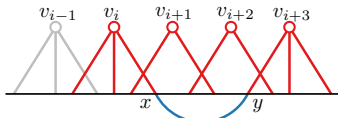
(d) Edge (x, y) is represented as outer edge.



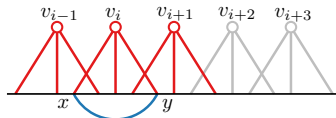
(e) Edge (x, y) is represented as outer edge.



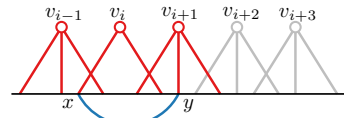
(f) Edge (x, y) is represented as outer edge.



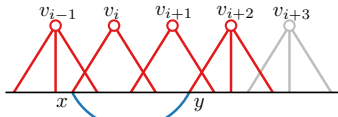
(g) The only possible case.



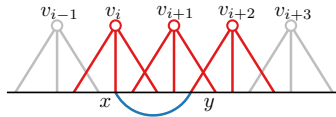
(h) Edge (x, y) represents a self-loop of G .



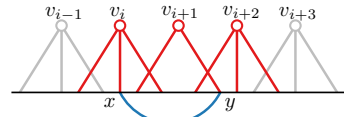
(i) Edge (x, y) is represented as outer edge.



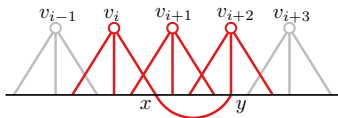
(j) Edge (x, y) is represented as outer edge.



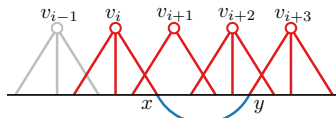
(k) The middle fan-bundle of v_{i+1} is redundant.



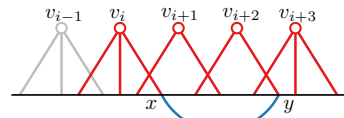
(l) Edge (x, y) is represented as outer edge.



(m) The middle fan-bundle of v_{i+1} is redundant.



(n) The middle fan-bundle of v_{i+2} is redundant.



(o) Edge (x, y) is represented as outer edge.

Figure 13: All different configurations in which x and y are: (a)-(g) at distance 3, and (h)-(o) at distance 4 along the outer face of H . The different subcases arise based on whether $e = (x, y)$ starts from the left, middle or right fan-bundle of vertex v_i of G , and on whether the vertices v_i, \dots, v_{i+3} have a middle fan-bundle or not. Note that the case illustrated in (g) is possible. For the remaining, the contradiction is given at the corresponding caption of each case.

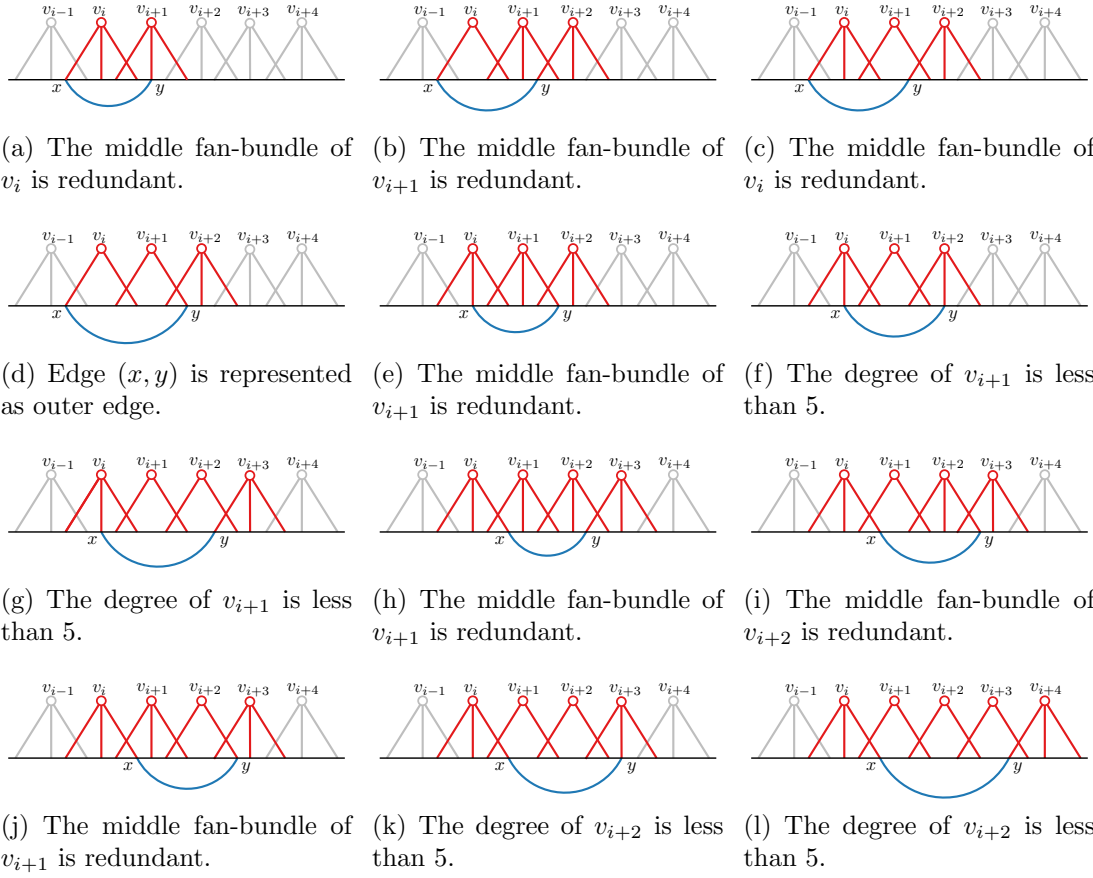


Figure 14: All different configurations in which x and y are at distance 5 along the outer face of H . The different subcases arise based on whether $e = (x, y)$ starts from the left, middle or right fan-bundle of vertex v_i of G , and on whether the vertices v_i, \dots, v_{i+3} have a middle fan-bundle or not. The contradiction is given at the corresponding caption of each case.

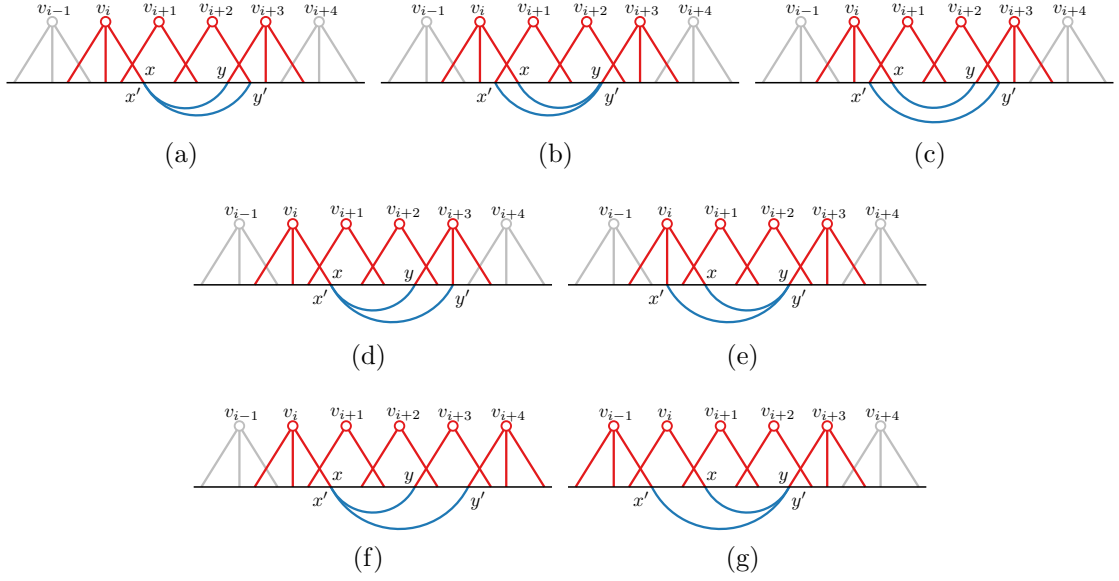


Figure 15: All different configurations in which x' and y' are: (a)-(b) at distance 4, and (c)-(g) at distance 5 along the outer face of H .

and y are at distance 3 along the outer face of H , it follows that x' and y' are at distance at least 4 along the outer face of H . By simplicity, it follows that x' and y' cannot be at distance 4 along the outer face of H ; see Figs. 15a and 15b. Thus, face f' has at least four vertices or equivalently x' and y' are at distance at least 5 along the outer face of H . Our next claim is that x' and y' cannot be at distance 5. To prove this claim, we distinguish two cases, based on whether one of x' and y' coincides with one of x and y , or not. In the first case, either $x' = x$ or $y' = y$ holds; see Figs. 15d-15g. Hence, either the degree of v_{i+2} or the degree of v_{i+1} is less than 5, which contradicts our assumption that every vertex has degree at least 5. In the second case, illustrated in Fig. 15c, edge e' represents edge (v_{i+1}, v_{i+2}) of G , which is already represented by an outer edge of H , and our claim follows. Finally, it is not difficult to observe that if x' and y' are at distance greater than 5 along the outer face of H , then either the degree of v_{i+2} or the degree of v_{i+1} is less than 5, which contradicts our assumption that every vertex has degree at least 5. This concludes the proof that f' cannot be of degree 2 in \mathcal{T} .

Let f_1, \dots, f_ℓ be the leaves of \mathcal{T} . Let also f'_1, \dots, f'_ℓ be the parents of f_1, \dots, f_ℓ in \mathcal{T} , respectively. Since f'_1, \dots, f'_ℓ cannot be of degree 2 in \mathcal{T} , it follows that $\ell \geq 3$. Furthermore, if $\ell = 3$, then \mathcal{T} must be a star with three leaves. This implies that H has exactly three inner edges, which is less than $2n + k - 9$, since $n \geq 7$. Hence, we may assume w.l.o.g. that $\ell \geq 4$ and therefore H has at most $(2n + k - 3) - 4 = 2n + k - 7$ inner edges. Note that if $\ell \geq 6$, then H has at most $(2n + k - 3) - 6 = 2n + k - 9$ inner edges. Hence, we only have to consider the case where $4 \leq \ell \leq 5$. We distinguish two cases: \mathcal{T} is a star or not. In the first case, H has either four or five inner edges, which is less than $2n + k - 9$, since $n \geq 7$. In the second case, there exist two faces in $\{f'_1, \dots, f'_\ell\}$ that are different from each other, say f'_1 and f'_ℓ . We prove that f'_1 cannot be a triangular face in H ; the proof for f'_ℓ is analogous. Note that this proof also completes the proof of our claim, as it directly implies that H cannot have more than $(2n + k - 3) - 4 - 2 = 2n + k - 9$ inner edges. Recall that f'_1 has at least two children in \mathcal{T} . Assume w.l.o.g. that f_1 and f_2 are children of f'_1 and let e_1 and e_2 be the unique inner edges incident to f_1 and f_2 , respectively. Since each of e_1 and e_2 must connect the right fan-bundle of a vertex v_i with the left fan-bundle of

vertex v_{i+3} as illustrated in Fig. 13g, it follows that e_1 and e_2 cannot share an endpoint. Hence, f'_1 is not triangular. This concludes the proof of the lemma. \square

We are now ready to prove the theorem about the edge density of 2-sided outer-1-fbp graphs.

Theorem 12. *A 2-sided outer-1-fbp graph G with n vertices has at most $4n - 9$ edges, where $n \geq 3$. This is a tight bound for all $n \geq 6$.*

Proof. Our proof is by induction on n . For the base case, observe that all graphs with $n \leq 6$ vertices have at most $n(n-1)/2 \leq 4n - 9$ edges. Since the complete graph K_6 is 2-sided outer-1-fbp (see Fig. 2c), it follows that all graphs with $n \leq 6$ vertices are in fact 2-sided outer-1-fbp.

For the inductive step, assume that G has $n \geq 7$ vertices and let Γ be a 2-sided outer-1-fbp drawing of G . Let also v_1, \dots, v_n be the vertices of G as they appear in clockwise order along the outer face of Γ . By the induction hypothesis, all 2-sided outer-1-fbp graphs with $n' < n$ vertices have at most $4n' - 9$ edges. We show that G has at most $4n - 9$ edges, as well.

We first consider the case in which there exists a vertex v_i , for some $i = 1, \dots, n$, with degree at most 4 in G . Since by the induction hypothesis the graph obtained by removing v_i and all its incident edges, has at most $4(n-1) - 9$ edges, we have that G has at most $4(n-1) - 9 + 4 = 4n - 9$ edges. Thus in the following we will assume that each vertex of G has degree at least 5.

As discussed above, we assume w.l.o.g. that the right fan-bundle of v_i crosses the left fan-bundle of v_{i+1} , and that the edge (v_i, v_{i+1}) is represented with a crossing-free unbundled part connecting their terminals.

We first consider the case in which there is a crossing between middle fan-bundles of two different vertices v_i and v_j ; see Fig. 11d. We can assume that v_i and v_j are not consecutive along the outer face of Γ , as otherwise these crossing middle fan-bundles would isolate the other two crossing fan-bundles of v_i and v_j (the right of v_i and the left of v_j , or vice versa), which could then be removed. Also, we can assume that the edge (v_i, v_j) belongs to G , as otherwise we can add it without violating the 2-sided outer-1-fan-bundle-planarity of G (see the dotted edge in Fig. 11d). This implies that there is a second pair of crossing fan-bundles on the other side of (v_i, v_j) , as otherwise we can add them (although we possibly do not use them; see the dashed fan-bundles in Fig. 11d). Thus, the edge (v_i, v_j) splits Γ into two 2-sided outer-1-fbp drawings Γ_1 and Γ_2 of two graphs G_1 and G_2 , both containing vertices v_i and v_j and the edge between them. Let n_1 and n_2 be the number of vertices in G_1 and G_2 , respectively; note that $n_1 + n_2 = n + 2$. By the induction hypothesis, Γ_1 and Γ_2 have at most $4n_1 - 9$ and $4n_2 - 9$ edges, respectively. Since (v_i, v_j) belongs to both Γ_1 and Γ_2 , we have that Γ has at most $(4n_1 - 9) + (4n_2 - 9) - 1 = 4(n + 2) - 19 = 4n - 11 < 4n - 9$ edges.

To complete the proof, we consider the case in which no pair of middle fan-bundles cross in Γ . In this case, we can assume w.l.o.g. that each vertex is incident to at most one middle fan-bundle, as otherwise we could merge all its middle fan-bundles into one. Hence, Lemmas 10 and 11 apply and we can conclude that H has at most $4n - 9$ edges. This also implies that G has at most $4n - 9$ edges, since the only edges that could be drawn in Γ without using fan-bundles are between consecutive vertices v_i and v_{i+1} , but these edges are already in H .

The fact that the bound is tight follows from Lemma 8. Hence, the statement follows. \square

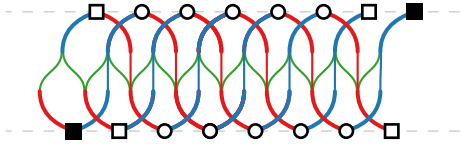


Figure 16: Illustration for the proof of Theorem 13.

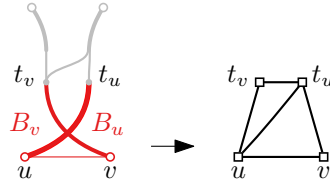


Figure 17: Illustration for the proof of Theorem 15.

In the following theorem, we study the edge density of 2-sided 2-layer 1-fbp graphs. The upper bound is an immediate consequence of Theorem 12. The corresponding lower bound is based on a construction similar to the one presented in the proof of Lemma 8.

Theorem 13. *A 2-sided 2-layer 1-fbp graph with $n \geq 3$ vertices has at most $3n - 7$ edges, while there exist 2-sided 2-layer 1-fbp graphs with $n \geq 10$ vertices and $2n - 4$ edges.*

Proof. Let G be a 2-sided 2-layer 1-fbp graph with $n \geq 3$ vertices. As in the proof of Theorem 7, we observe that one can add $n - 2$ edges in G and obtain a new graph G' that is 2-sided outer-1-fbp. Since by Theorem 12 graph G' cannot have more than $4n - 9$ edges, it follows that G cannot have more than $3n - 7$ edges. For the corresponding lower bound, observe that all vertices of the graph of Fig. 16 have degree exactly 4, except for the vertices drawn as filled and non-filled squares, which have degrees 2 and 3, respectively. Hence, this graph has in total $2n - 4$ edges. \square

For the general case, we have given in Lemma 9 a lower bound on the edge density. In the following, we focus on a linear upper bound.

Consider a 2-sided 1-fbp drawing Γ of a maximally dense graph G , which contains the maximum number of uncrossed edges. Let n and m be the number of vertices and edges of G , respectively. To give an upper bound for m , we observe that each edge of G can be identified by its unbundled part in Γ , which is unique for each edge.

We proceed by defining a planar auxiliary subgraph G_p of G , with n_p vertices and m_p edges, as follows. Graph G_p has the same vertex set as G , and so $n_p = n$, and contains all uncrossed edges of G in Γ . Since Γ contains a maximum number of uncrossed edges, it follows that for each pair of crossing fan-bundles B_u and B_v , graph G_p contains the base edge (u, v) of B_u and B_v (note that the base edge of B_u and B_v might occur several times in G_p , but such copies are pairwise non-homotopic). Hence, by the Euler's formula for planar graphs, it follows that $m_p \leq 3n - 6$.

Next, we create another planar graph G'_p , with n'_p vertices and m'_p edges, consisting of the vertices of G and the terminals of the fan-bundles of Γ , which we call *terminal vertices*. For each pair of crossing fan-bundles B_u and B_v with terminals t_u and t_v , graph G'_p contains edges (u, t_v) , (t_v, t_u) , (t_u, v) , and either edge (u, t_u) or edge (v, t_u) ; see Fig. 17. We refer to these edges as *bridging edges*, since they bridge vertices of the original graph with terminal vertices. Finally, for each unbundled part of each edge in Γ , graph G'_p has an edge connecting the corresponding terminal vertices of G'_p . By construction, graph G'_p is planar. If we denote by t the number of terminal vertices of G'_p , then $n'_p = n + t$ and since G'_p is planar $m'_p \leq 3(n + t) - 6$ holds.

Observe, however, that for each pair of terminal vertices t_u and t_v corresponding to the terminals of two crossing fan-bundles anchored at two vertices u and v , respectively, all the four bridging edges incident to t_u and t_v are not in correspondence with edges of the original graph G . Hence, the number of edges that actually correspond to distinct

edges of G is equal to m'_p minus the number of bridging edges, which is equal to $2t$ since every two terminal vertices determine four bridging edges. This implies that:

$$m \leq 3(n+t) - 6 - 2t = 3n + t - 6 \quad (1)$$

Note that the arguments presented so far would already give a linear upper bound on the number of edges of G ; in fact, since we can associate at most four terminal vertices to each edge of G_p (as each of these edges can have at most two crossing fan-bundles on each side), we have that $t \leq 4m_p$, which gives $t \leq 4 \cdot (3n - 6) = 12n - 24$ and thus $m \leq 3n + t - 6 \leq 15n - 30$.

In order to improve this bound, we will show in the following that the value of m_p is actually significantly smaller than $3n - 6$. The general idea is that, if G_p contains a small face f (which is always the case if m_p is equal or close to $3n - 6$), then it is not possible for all the edges incident to f to have fan-bundles inside f without having multiple edges in G ; note that this reduces the number of terminal vertices in G'_p , and hence its number of edges. This is clear, for example, when f is triangular, and thus all the connections that could be represented by fan-bundles inside f are already represented by the three edges incident to f ; in this case, in fact, none of these three edges incident to f may have fan-bundles inside it. We formalize this concept in the following.

Consider any (possibly non-simple) k -cycle of G_p , with $2 \leq k \leq 6$, delimiting a face of some connected component of G_p in Γ . If this k -cycle also delimits a face of G_p , then we call it *empty*; otherwise we call it *non-empty*. Note that if $k = 2$ then the cycle must be non-empty (as otherwise we would have a pair of homotopic parallel edges). Also note that a non-empty k -cycle contains in its interior all the vertices and edges of at least another connected component of G_p . Further, there exists a non-connected face of G_p whose boundary consists of this non-empty k -cycle and the outer boundaries of all the components contained in it. We denote by f_k the number of empty k -cycles and by ϕ_k the number of non-empty k -cycles in Γ . Hence, $\sum_{k=3}^{\infty} f_k$ and $\sum_{k=2}^{\infty} \phi_k$ are the numbers of connected and non-connected faces of G_p , respectively.

For the following lemma, recall that an edge is accounted twice for a face if both its sides are incident to this face.

Lemma 14. *For a non-empty k -cycle C with $k = 2, 3, 4$, the face f of G_p that is delimited by C has at least 5 incident edges.*

Proof. In order to prove the statement for $k = 3, 4$, it is sufficient to show that at least one connected component of G_p in the interior of C is not an isolated vertex. By maximality, in Γ there must be a crossing of two fan-bundles in the interior of C . Let these crossing fan-bundles be anchored at vertices u and v . Recall that G_p contains the edge (u, v) , since it is the base edge of this bundle crossing. This implies that either both u and v belong to C or none of them belongs to C . In the latter case u and v belong to a connected component of G_p in the interior of C which is not an isolated vertex and the statement follows. So we may assume that for every fan-bundle crossing, the base edge is an edge of C . Consider the graph H induced by the isolated vertices in the interior of C and by the terminals of the fan-bundles whose base edges are edges of C . By our previous observation this graph is plane. Note that when $k = 3$ there is no edge in H between two terminals, as otherwise any such edge would represent an edge of C ; a contradiction. On the other hand, when $k = 4$, there can be at most two edges connecting terminal vertices in H (corresponding to the two diagonals of C ; see Fig. 18a). In both cases, we conclude that there is at least one isolated vertex in the interior of C that is incident to the outer face of H . Hence, this vertex can be connect to a vertex of C with a planar edge; a contradiction.

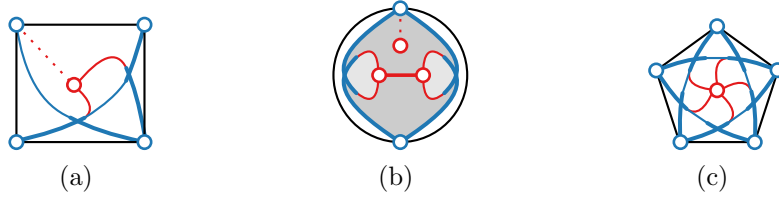


Figure 18: Illustrations for the proof of Lemma 14.

Consider now the case $k = 2$. Let u and v be the two vertices belonging to C . Using the same argument as above, we can conclude that there exists at least a connected component of G_p in the interior of C that is not an isolated vertex. If this component has at least three edges incident to its outer face then the statement follows. The same holds if there exists more than one component that is not an isolated vertex. Hence we can conclude that there exists a single component σ that is not an isolated vertex, and that either σ is an edge or its outer face is a pair of parallel edges. In both cases, σ has only two vertices w and z incident to its outer face. If there is no isolated vertex in f then u, v, w and z are the only vertices incident to f . This contradicts the fact that the pairs $\langle u, v \rangle$ and $\langle w, z \rangle$ belong to different components of G_p , since at least one of the vertices w or z can be connected to u or v by a planar edge. So we can assume that there exists an isolated vertex incident to f . Since the isolated vertices are not incident to fan-bundles and since edges (u, v) and (w, z) are planar, the only possible connections between two terminals in f are between a terminal of a fan-bundle anchored at u or v and a terminal of a fan-bundle anchored at w or z . These connections split f into at most 4 regions (refer to the gray colored regions of Fig. 18b). Since each of these regions contains on its boundary at least one of the vertices u, v, w or z , it is always possible to connect an isolated vertex to one of these four vertices by a planar edge; a contradiction.

We conclude the proof by noting that for $k = 5$ it is possible to have a non-empty k -cycle that contains in its interior only isolated vertices; for an illustration refer to Fig. 18c. \square

In the following we will assume that every empty k -cycle with $3 \leq k \leq 6$ has no terminal vertex in its interior. We observe that for $k \neq 3$ this results in an underestimation of the number of edges, which we will compensate in the final computation by considering each of the cases independently.

This assumption implies that the number t of terminal vertices may be smaller than $4m_p$, and in particular it can be expressed as

$$t \leq 4m_p - 6f_3 - 8f_4 - 10f_5 - 12f_6 \quad (2)$$

Further, we can also express m_p as a function on the number of the k -cycles. In particular, by using the fact that $2m_p$ equals the sum of the size of all faces of G_p , and by using Euler's formula for disconnected planar graphs $m_p = n + f_p - 1 - c_p$, where f_p denotes the number of faces of G_p and c_p denotes the number of its connected components, we get:

$$\begin{aligned} & 3f_3 + 4f_4 + 5(f_5 + \phi_2 + \phi_3 + \phi_5) + 6(f_6 + \phi_4 + \phi_6) \\ & + 7(f_p - (\phi_2 + f_3 + \phi_3 + f_4 + \phi_4 + f_5 + \phi_5 + f_6 + \phi_6)) \\ & \leq 2m_p = 2n + 2f_p - 2 - 2c_p \end{aligned}$$

where we use the coefficient 5 for ϕ_2 and ϕ_3 and the coefficient 6 for ϕ_4 due to Lemma 14. This yields:

$$5f_p - 4f_3 - 3f_4 - 2(f_5 + \phi_2 + \phi_3 + \phi_5) - (f_6 + \phi_4 + \phi_6) \leq 2n - 2 - 2c_p \quad (3)$$

Observe that $c_p \geq \phi_2 + \phi_3 + \phi_4 + \phi_5 + \phi_6$, since each connected component of G_p can be used to identify at most one face as non-empty. Thus, replacing c_p in Eq. 3 we obtain:

$$\begin{aligned} & 5f_p - 4f_3 - 3f_4 - 2(f_5 + \phi_2 + \phi_3 + \phi_5) - (f_6 + \phi_4 + \phi_6) \\ & \leq 2n - 2 - 2(\phi_2 + \phi_3 + \phi_4 + \phi_5 + \phi_6) \end{aligned}$$

which yields:

$$f_p \leq \frac{1}{5}(2n - 2 + 4f_3 + 3f_4 + 2f_5 + f_6)$$

Applying again Euler's formula $m_p \leq n + f_p - 2$ (using that $c_p \geq 1$), we obtain:

$$m_p \leq \frac{1}{5}(7n - 12 + 4f_3 + 3f_4 + 2f_5 + f_6)$$

By Eq. 2 we have:

$$t \leq \frac{4}{5}(7n - 12 + 4f_3 + 3f_4 + 2f_5 + f_6) - 6f_3 - 8f_4 - 10f_5 - 12f_6,$$

which implies:

$$t \leq \frac{1}{5}(28n - 48 - 14f_3 - 28f_4 - 42f_5 - 56f_6)$$

Hence, by Eq. 1 we might provide a bound for m , which is unfortunately underestimated, as we observed above:

$$m \leq 3n + t - 6 = \frac{1}{5}(43n - 78 - 14f_3 - 28f_4 - 42f_5 - 56f_6)$$

To compensate the underestimation of the number of edges, we conclude our discussion by studying how many crossing edges can be drawn in the interior of an empty k -cycle, for $k = 3, \dots, 6$. Namely, empty 3-cycles (that is, triangular faces) cannot have any edge in their interior, as discussed above. Empty 4-cycles can have at most two edges, namely those connecting vertices at distance 2 along the 4-cycle. For the number of edges of empty k -cycles with $k = 5, 6$, we use as an upper bound the number of edges in the complete graph on k vertices minus k . We thus have five edges for $k = 5$ and ten edges for $k = 6$. Hence, the final bound for the number of edges of G is:

$$m \leq 3n + t - 6 + 2f_4 + 5f_5 + 10f_6 = \frac{1}{5}(43n - 78 - 14f_3 - 18f_4 - 17f_5 - 6f_6)$$

Hence, G cannot have more than $(43n - 78)/5$ edges. Combining with the lower bound we proved in Lemma 8, we obtain the following theorem.

Theorem 15. *A 2-sided 1-fbp graph with $n \geq 3$ vertices has at most $(43n - 78)/5$ edges, while there exist 2-sided 1-fbp graphs with $n \geq 9$ vertices and $6n - 18$ edges.*

6 NP-completeness

In this section, we prove that the problem of testing whether a graph G with a given rotation system R admits a 1-sided or a 2-sided 1-fbp drawing preserving R is NP-complete. We present the reduction for the 1-sided model in detail, and we only highlight the differences for the 2-sided model.

Theorem 16. *Given a graph G and a fixed rotation system R of G , it is NP-complete to decide whether G admits a 1-sided 1-fbp drawing preserving R .*

Proof. Membership in NP can be proved as for fan-planarity [6], which is in turn inspired by the corresponding proof for the crossing number [24].

We prove the NP-hardness by means of a reduction from problem 3-PARTITION. The idea is based on a general scheme proposed by Bekos et al. [6] to prove the NP-completeness of the fan-planarity problem with a fixed rotation system. Recall that an instance $\langle A, B \rangle$ of 3-PARTITION consists of an integer B and of a set $A = \{a_1, a_2, \dots, a_{3m}\}$ of $3m$ integers such that $a_i \in (\frac{B}{4}, \frac{B}{2})$, for $i = 1, 2, \dots, 3m$, and $\sum_{i=1}^{3m} a_i = mB$. Problem 3-PARTITION asks whether A can be partitioned into m subsets A_1, A_2, \dots, A_m , each of cardinality 3, such that the sum of the numbers in each subset is exactly B . Note that 3-PARTITION is strongly NP-hard [23]. So, we may assume w.l.o.g. that B is bounded by a polynomial in m .

Given an instance $\langle A, B \rangle$ of 3-PARTITION, we show how to construct in polynomial time an instance $\langle G, R \rangle$ of our problem such that there is a solution for $\langle A, B \rangle$ if and only if G admits a 1-sided 1-fbp drawing preserving R .

Central in our transformation is the so-called *barrier gadget*. To describe this gadget, we first introduce a graph H composed of seven vertices a, b, c, d, e, f, g ; refer to Fig. 19a. Graph H contains cycle (a, b, c, d, e, f) , which is called *boundary cycle* and whose edges are the *boundary edges* of H , and two edges (c, g) and (f, g) . Also, for each vertex $u \in \{c, f, g\}$ and for each vertex $v \in \{a, b, d, e\}$, graph H contains edge (u, v) . The rotation system of H is such that the boundary cycle delimits its outer face in any drawing respecting this rotation system, while all the other edges (which are called *inner edges*) are routed in its interior, as in Fig. 19a. We refer to vertices a, e , and f as *left-sided* and to b, c , and d as *right-sided*.

To construct an n -vertex barrier gadget with $n \geq 7$, we employ $\lfloor (n-3)/4 \rfloor$ copies of the graph H , which we glue with each other by identifying the left-sided vertices of one copy with the right-sided vertices of the next copy; see Fig. 19b. We fix the rotation system of the barrier gadget so that for each vertex, the edges belonging to the same copy of H are consecutive around it. We will use the barrier gadget in order to constrain the routes of some specific paths of G .

Consider now a biconnected 1-sided 1-fbp graph G with rotation system R that contains as a subgraph a barrier gadget G_b . Let Γ be any 1-sided 1-fbp drawing of G respecting R . Observe that, by the choice of the rotation system, the boundary edges of G_b do not cross any other edge of G_b , while all the inner edges have at least one crossing with another inner edge, except possibly for those incident to g . In particular, the inner edges incident to a must share a fan-bundle anchored at a , and those incident to b must share a fan-bundle anchored at b , and these two fan-bundles must cross; analogously, two fan-bundles anchored at d and e must cross. This implies that no path π of $G \setminus G_b$ can enter inside the boundary cycle of G_b and cross an inner edge of G_b in Γ . On the other hand, if path π enters inside the boundary cycle of G_b without crossing any inner edge, then it must cross the same boundary edge a second time to exit this cycle (due to the biconnectivity

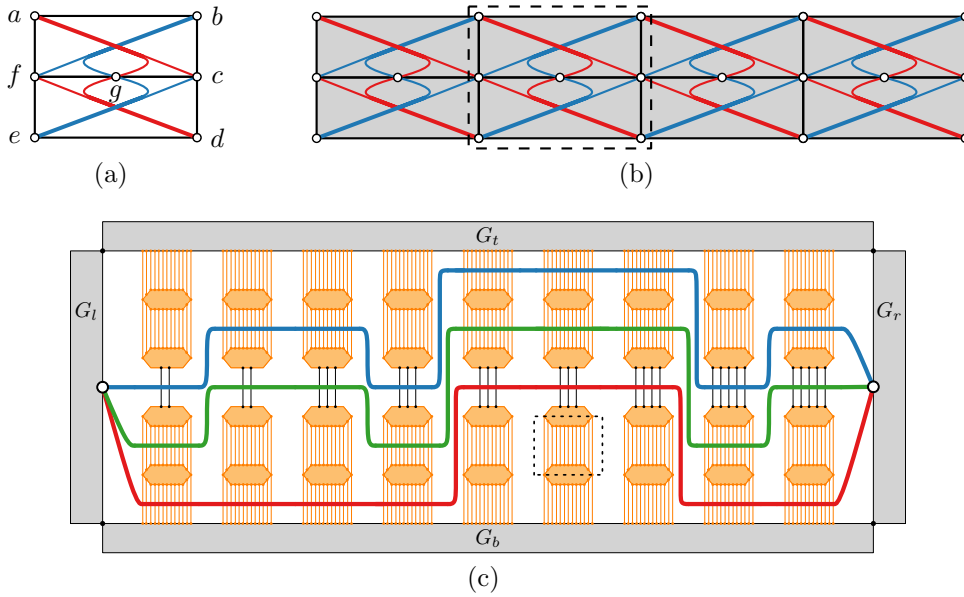


Figure 19: (a) The graph H used in the construction of the barrier gadget, which is illustrated in (b). In (c) we provide the whole scheme of the reduction from 3-PARTITION, for the case in which $m = 3$, $A = \{2, 2, 2, 3, 3, 3, 4, 5, 6\}$, and $B = 10$. The transversal paths are routed according to the following solution of 3-PARTITION: $A_1 = \{2, 3, 5\}$, $A_2 = \{2, 3, 5\}$, and $A_3 = \{3, 3, 4\}$. The hexagonal regions are the obstacles; the dotted rectangle contains all the vertical edges of a (bottom) cell.

of G). In other words, if a path π enters G_b in Γ , then it must exit it by using the same boundary edge, which is equivalent to not entering it at all.

We construct an instance $\langle G, R \rangle$ of our problem based on an instance $\langle A, B \rangle$ of 3-PARTITION as follows. We start our construction with the *wall gadget*, which consists of a cyclic chain of four barrier gadgets G_t , G_r , G_b , and G_l that surrounds the whole construction; see Fig. 19c. The barrier gadgets G_t and G_b are called *top* and *bottom beams*, respectively, and contain exactly $4 \cdot (3mK + 1) + 3$ vertices each, where K is a large integer number, e.g., $K = B^2$. The barrier gadgets G_l and G_r are called *left* and *right walls*, respectively, and have only 11 vertices each. In other words, G_t and G_b contain $3mK + 1$ copies of H , while G_l and G_r contain only two copies of H . By the choice of the rotation system R and of the vertices shared by two consecutive barrier gadgets, we may assume that $3mK$ vertices of each of G_t and G_b , and one vertex of each of G_l and G_r , are incident to the *interior of the wall*, that is, the closed region delimited by the wall gadget.

The top and bottom beams are “bridged” to each other by a set of $3m$ *columns*; see Fig. 19c for an illustration of the case $m = 3$. Each *column* contains $2m - 1$ *cells*, where a cell consists of a set of pairwise disjoint edges, called *vertical edges* of that cell (see, e.g., the edges that are contained in the dotted rectangle in Fig. 19c). There are $m - 1$ *top cells*, one *central cell*, and $m - 1$ *bottom cells*. Cells of the same column are separated by $2m - 2$ barrier gadgets, called *obstacles*, which have $4 \cdot (K - 1) + 3$ vertices each (see the hexagonal regions in Fig. 19c). The number of vertical edges of each of the $3m$ central cells depends on the elements of instance A . In particular, for $i = 1, 2, \dots, 3m$, the central cell C_i of the i -th column has exactly a_i vertical edges connecting its delimiting obstacles. Each of the remaining cells has K vertical edges. Hence, each of the top and bottom cells contains significantly more vertical edges than any central cell. We say that central cells are *sparse*, while the top and the bottom cells are *dense*.

The left and the right walls are “bridged” to each other by a set of m pairwise internally disjoint paths $\pi_1, \pi_2, \dots, \pi_m$, called *transversal paths*, which all originate from the same vertex of the left wall, called *origin*, and terminate at the same vertex of the right wall, called *destination*. Each of these paths has length $(3m - 3)K + B$.

Regarding the choice of the rotation system R , we define a cyclic order of the edges around each vertex that conforms with the following constraints.

- C.1: all inner edges of each barrier gadget lie in the interior of its boundary cycle,
- C.2: the wall gadget is embedded such that $3mK + 2$ vertices of each top and bottom beam and four vertices of each left and right wall are incident to the interior of the wall,
- C.3: all columns can be embedded in the interior of the wall without crossing each other,
- C.4: the vertical edges of each cell can be embedded without crossing each other, and
- C.5: the order of the edges of the transversal paths around the origin is the reverse of the corresponding order around the destination, which guarantees that the transversal paths can avoid crossing each other.

This concludes our construction, which is clearly polynomial in m , since we have assumed that B is bounded by a polynomial in m .

We now prove the equivalence, which is mainly based on the observation that each transversal path has to cross exactly 3 sparse cells and exactly $3m - 3$ dense cells in any 1-sided 1-fbp drawing. This is due to the following fact. Since each transversal path has length $(3m - 3)K + B$, it can cross at most $3m - 3$ dense cells in order to connect the origin to the destination. On the other hand, since no two different paths can cross the same cell in any 1-sided 1-fbp drawing, we have that if any transversal path crosses fewer than $3m - 3$ dense cells, then there must be another one that crosses more than $3m - 3$ of these cells, and the claim follows.

Suppose that the set A admits a partition into subsets A_1, A_2, \dots, A_m , each composed of three integers summing up to B . If one omits the transversal paths, then it is easy to compute a 1-sided 1-fbp drawing Γ of G preserving R . It is essentially a drawing like the one depicted in Fig. 19c, where columns are next to each other in the interior of the wall. To complete the drawing, we embed the transversal paths $\pi_1, \pi_2, \dots, \pi_m$ of G in the partial drawing of G constructed so far under the following requirements:

- R.1 transversal paths $\pi_1, \pi_2, \dots, \pi_m$ do not cross each other,
- R.2 transversal paths $\pi_1, \pi_2, \dots, \pi_m$ do not cross any barrier gadget,
- R.3 each cell is traversed by at most one transversal path (as otherwise 1-sided 1-fan-bundle-planarity would be deviated), and
- R.4 each transversal path passes through exactly 3 sparse cells and $3m - 3$ dense cells.

We obtain a drawing satisfying these requirements as follows. For $j = 1, 2, \dots, m$, let $A_j = \{a_\kappa, a_\lambda, a_\mu\}$, where $1 \leq \kappa, \lambda, \mu \leq 3m$. Then, in the drawing Γ , the path π_j will cross the κ -th, λ -th, and μ -th vertical columns of G through sparse cells, and the remaining vertical columns of G through dense cells. Hence, Requirement R.4 is satisfied. The routing of the remaining transversal paths through the κ -th vertical column is done as follows. By construction, there exist $m - 1$ cells above and $m - 1$ cells below the sparse cell

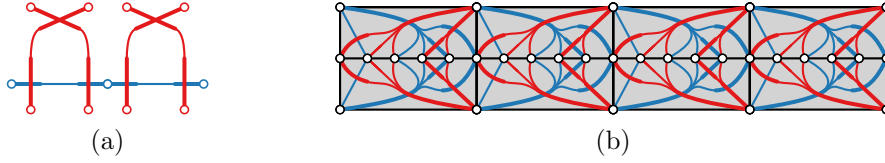


Figure 20: (a) Edges in the same cell in the 2-sided model, and (b) the barrier gadget in the 2-sided models.

of the κ -th vertical column (all of which are dense). Hence, there exist at least as many available dense cells as transversal paths to route at each side of the sparse cell of the κ -th vertical column. Hence, we can route the remaining transversal paths through the κ -th vertical column such that Requirements R.1–R.3 are also satisfied. The corresponding routings through the λ -th and μ -th vertical columns of G are symmetric. This implies that the drawing Γ of G is indeed 1-sided 1-fbp and preserves R .

Suppose now that G admits a 1-sided 1-fbp drawing Γ preserving the rotation system R . As already mentioned, each of the transversal paths crosses exactly 3 sparse cells and exactly $3m - 3$ dense cells. In addition, 1-sided 1-fan-bundle-planarity ensures that no two transversal paths pass through the same cell. With these two properties, we can construct a solution A_1, A_2, \dots, A_m of instance $\langle A, B \rangle$ of 3-PARTITION as follows. Assume that path π_j crosses the κ -th, λ -th, and μ -th vertical columns of Γ through sparse cells, where $1 \leq \kappa, \lambda, \mu \leq 3m$. Then, the j -th partition set A_j of instance $\langle A, B \rangle$ of 3-PARTITION will contain integers $\{a_\kappa, a_\lambda, a_\mu\}$. Since $a_\kappa + a_\lambda + a_\mu = B$, the solution constructed this way is indeed a solution of 3-PARTITION for the instance $\langle A, B \rangle$. This concludes our NP-hardness reduction. \square

We observe that the NP-completeness of 2-sided 1-fan-bundle-planarity with a given rotation system can be proved as in Theorem 16 with the following modifications. Since each edge of the transversal path can be crossed twice in the 2-sided model, we double the number of vertical edges in the dense and sparse cells. To avoid that two transversal paths cross the same cell, we enforce that consecutive pairs of edges in the same cell cross; see Fig. 20a. For the barrier gadget, we use the graph of Fig. 20b, which by the choice of the rotation system cannot be crossed by any transversal path. We summarize these observations in the following theorem.

Theorem 17. *Given a graph G and a fixed rotation system R of G , it is NP-complete to determine whether G admits a 2-sided 1-fbp drawing preserving R .*

7 Recognition and drawing algorithms

In this section, we present recognition and drawing algorithms for biconnected 1-sided 2-layer 1-fbp graphs, maximal 1-sided 2-layer 1-fbp graphs, and triconnected 1-sided outer-1-fbp graphs. We also give a complete characterization of general 1-sided 2-layer 1-fbp graphs.

7.1 1-sided 2-layer 1-fan-bundle-planar graphs.

In this subsection, we present linear-time recognition and drawing algorithms for biconnected 1-sided 2-layer 1-fbp graphs and maximal 1-sided 2-layer 1-fbp graphs. Since a 1-sided 2-layer 1-fbp graph is by definition 2-layer fan-planar, naturally our results build

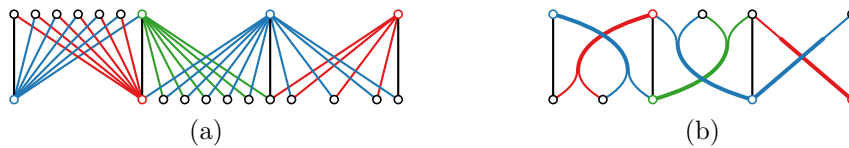


Figure 21: Illustration of (a) a snake and (b) a baby snake.

upon known results by Binucci et al. [7] for 2-layer fan-planar graphs, who showed that a biconnected bipartite graph is maximal 2-layer fan-planar if and only if it is a *snake*, i.e., a chain of graphs G_1, \dots, G_k such that each G_i is a complete bipartite graph K_{2,h_i} , $h_i \geq 2$ that shares a pair of vertices, called *merged vertices*, with G_{i+1} , and no vertex is shared by more than two graphs; see Fig. 21 for an illustration. Furthermore, they also showed that a biconnected bipartite graph is 2-layer fan-planar if and only if it is a spanning subgraph of a snake. Hence, every biconnected 2-layer 1-fbp graph has to be a spanning subgraph of a snake. However, not every snake is 1-sided 2-layer 1-fbp, as we demonstrate in the following lemma.

Lemma 18. *The complete bipartite graph $K_{2,3}$ is 1-sided 2-layer 1-fan-bundle-planar, while the complete bipartite graph $K_{2,4}$ is not 1-sided 2-layer 1-fan-bundle-planar.*

Proof. Let $\{a_1, a_2\}$ and $\{b_1, b_2, b_3\}$ be the two partition sets of $K_{2,3}$. Topologically, there is exactly one 1-sided 2-layer 1-fbp drawing of $K_{2,3}$ such that $x(a_1) < x(a_2)$ and $x(b_1) < x(b_2) < x(b_3)$, which is illustrated in Fig. 22. The reason is that any 2-layer drawing of $K_{2,3}$ is not crossing-free, which implies that a_1 and a_2 are the anchors of two fan-bundles B_{a_1} and B_{a_2} that cross. Note that the crossing can potentially be realized by two fan-bundles B_{b_1} and B_{b_3} anchored at b_1 and b_3 , respectively. However, in this case B_{b_1} and B_{b_3} would prevent any connection to b_2 .

We now prove that the complete bipartite graph $K_{2,4}$ is not 1-sided 2-layer 1-fbp. Let $\{a_1, a_2\}$ and $\{b_1, b_2, b_3, b_4\}$ be the two partition sets of $K_{2,4}$. Since the complete bipartite graph $K_{2,3}$ induced by a_1, a_2, b_1, b_2 , and b_3 has a unique 1-sided 2-layer 1-fbp drawing, it suffices to prove that it is not possible to add vertex b_4 to this drawing and to connect it to both a_1 and a_2 without violating its 1-sided 2-layer 1-fan-bundle-planarity; we assume as above that $x(a_1) < x(a_2)$ and $x(b_1) < x(b_2) < x(b_3)$. By symmetry, we only have to consider two cases: $x(b_4) < x(b_1)$ and $x(b_1) < x(b_4) < x(b_2)$. In the first case, b_4 cannot be connected to a_2 , as this connection would cross two fan-bundles incident to a_1 . In the second case, b_4 cannot be connected to a_1 , as this connection would cross an unbundled part of an edge incident to a_2 . \square

Since Binucci et al. [7] showed that a biconnected bipartite graph is 2-layer fan-planar if and only if it is a spanning subgraph of a snake, Lemma 18 immediately leads to a characterization of biconnected 2-layer 1-fbp graphs; see Lemma 19. We say that a snake is a *baby snake* if each graph in its chain is a $K_{2,2}$ or a $K_{2,3}$; see Fig. 21b for an example.

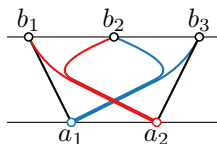


Figure 22: A 1-sided 2-layer 1-fbp drawing of $K_{2,3}$.

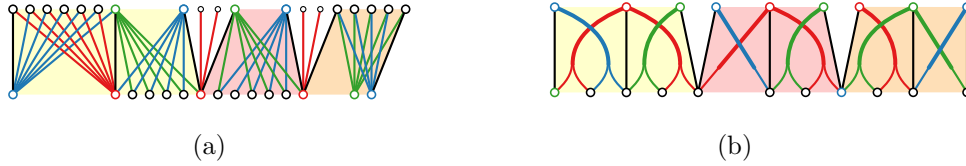


Figure 23: Illustration of (a) a stegosaurus and (b) a baby stegosaurus.

Lemma 19. *A biconnected bipartite graph is 2-layer 1-fan-bundle-planar if and only if it is a spanning subgraph of a baby snake.*

A direct consequence of the aforementioned characterization is that we can recognize (and in the case of an affirmative answer also draw) these graphs, by employing the corresponding recognition (and drawing, respectively) algorithm by Binucci et al. [7]. We summarize this observation in the following theorem.

Theorem 20. *Biconnected 1-sided 2-layer 1-fan-bundle-planar graphs can be recognized and drawn in linear time.*

In the remainder of this subsection, we relax biconnectivity and require maximality. Binucci et al. [7] showed that a bipartite graph is maximal 2-layer fan-planar if and only if it is a *stegosaurus*, that is, a chain of snakes that are connected at *common cutvertices*, where each common cutvertex is incident to exactly two snakes, plus a set of degree-1 vertices, called *legs*, each of which is attached to a common cutvertex; see Fig. 23a for an illustration. The following lemma has been proven by Binucci et al. [7], but the proof also works without modification for our model.

Lemma 21 (Binucci et al. [7]). *In any 1-sided 2-layer 1-fan-bundle-planar drawing, no biconnected component of a graph can be crossed by an independent edge.*

By Lemma 21, it follows that the biconnected components in a 2-layer 1-fbp drawing are placed next to each other without crossings. In the following lemma, we describe the structure of maximal 1-sided 2-layer 1-fbp graphs without legs. To this end, we need the following definition. We call a stegosaurus a *baby stegosaurus* if its snakes are baby snakes and if it contains no legs; see Fig. 23b for an example. Note that a baby stegosaurus can be drawn 1-sided 2-layer 1-fbp by just drawing its snakes independently, then connecting them via their common cutvertices.

Lemma 22. *If we remove the legs of a maximal 1-sided 2-layer 1-fan-bundle-planar graph, then we obtain a baby stegosaurus.*

Proof. Since every biconnected component of a maximal 1-sided 2-layer 1-fbp graph is a baby snake, the lemma holds as long as there exist no bridges. If this is not the case, by Lemma 21 any two components separated by a bridge are drawn without crossing each other. If the bridge is planar, then we can connect the two components by another edge that crosses the bridge. On the other hand, if the bridge is crossed by a fan-bundle, then we can connect the origin of this fan-bundle to the other component by crossing the bridge. In both cases, we obtain a contradiction to the graph’s maximality. \square

Note that in a maximal 2-layer fan-planar graph, there exist no legs. In fact, Binucci et al. [7] showed that a leg contained in a 2-layer fan-planar graph is incident to a $K_{2,h}$, which in turn can be augmented to a $K_{2,h+1}$ by adding an additional edge without

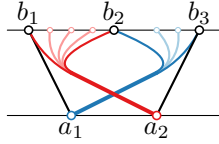


Figure 24: Legs inside a $K_{2,3}$.

affecting fan-planarity. In our case, however, a $K_{2,3}$ cannot be augmented to a $K_{2,4}$ in the presence of a leg (due to Lemma 18), and therefore Lemma 22 does not immediately yield a characterization of maximal 1-sided 2-layer 1-fbp graphs. So, in the following, we investigate to which vertices the legs of a maximal 1-sided 2-layer 1-fbp graph can be attached.

To this end, let G be a maximal 1-sided 2-layer 1-fbp graph and let Γ be a 2-layer 1-fbp drawing of G . Since by Lemma 22, graph G is a baby stegosaurus containing legs. We refer to the $K_{2,2}$ and $K_{2,3}$ subgraphs composing the baby snakes of G as *components* of G .

First, consider a $K_{2,3}$ component of G with partitions $\{a_1, a_2\}$ and $\{b_1, b_2, b_3\}$ and assume w.l.o.g. that $x(a_1) < x(a_2)$ and $x(b_1) < x(b_2) < x(b_3)$ in drawing Γ ; see Fig. 22. There are no legs attached to b_1 , b_2 and b_3 that lie between a_1 and a_2 in Γ , because the interval between a_1 and a_2 is “blocked” by the fan-bundles anchored at a_1 and a_2 . However, G may have any number of legs attached to a_1 and a_2 that lie between b_2 and b_3 , and between b_1 and b_2 , respectively; see Fig. 24.

In the following lemma, we focus on legs attached to vertices of a $K_{2,2}$ component of G .

Lemma 23. *There exist no leg in G that is attached to a vertex that belongs to a $K_{2,2}$ component of G .*

Proof. Consider a $K_{2,2}$ component of G with partition sets $\{a_1, a_2\}$ and $\{b_1, b_2\}$, such that $x(a_1) < x(a_2)$ and $x(b_1) < x(b_2)$ holds in Γ ; see Figs. 25a and 25b. Note that any 2-layer drawing of $K_{2,2}$ is not crossing-free. Hence, it must contain two fan-bundles that cross. Assume w.l.o.g. that one fan-bundle is anchored at a_1 . Then, the other fan-bundle is either anchored at a_2 or at b_1 , since anchoring it at b_2 is not possible.

We will first prove that there exist no leg in G that lies between a_1 and a_2 , or between b_1 and b_2 in Γ . For a proof by contradiction, assume that there exists such a leg. We first consider the case in which the two fan-bundles are anchored at a_1 and a_2 ; see Fig. 25c. In this case, there exists no leg incident to b_1 and b_2 that lies between a_1 and a_2 . Hence, there exists at least one leg attached to either a_1 or a_2 , say to the former, that lies between b_1 and b_2 in Γ . Then, the maximality of G is contradicted, as it is possible to add an edge between the leftmost such leg and a_2 without violating the 1-fan-bundle-planarity of Γ .

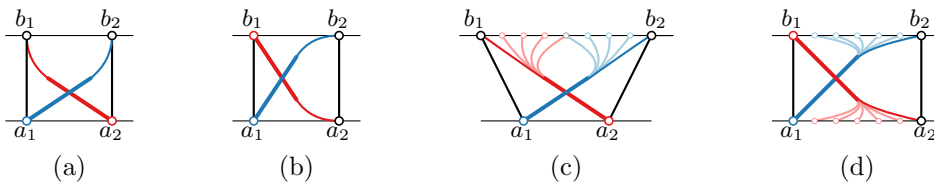


Figure 25: (a)-(b) The two ways to attach the fan-bundles inside a $K_{2,2}$, (c) all legs are attached to a_1 and a_2 , and (d) all legs are attached to a_1 and b_1 .

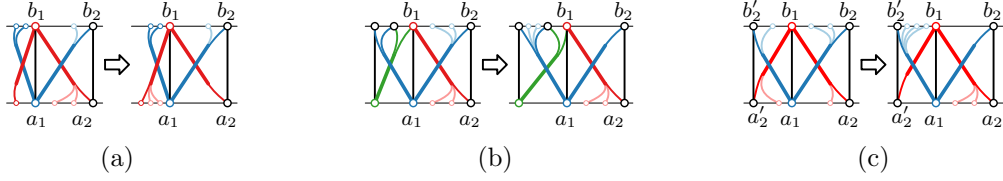


Figure 26: Proof that there is no leg attached to a_1 that lies between b_1 and b_2 : (a) b_1 and b_2 are the only neighbors of a_1 that belong to some component of G , (b) a_1 and b_1 belong to a $K_{2,3}$ component, and (c) a_1 and b_1 belong to a second $K_{2,2}$ component.

We now consider the case in which the two fan-bundles are anchored at a_1 and b_1 ; see Fig. 25d. Observe that there exists no leg in G attached to a_2 or b_2 that lies between b_1 and b_2 , and between a_1 and a_2 , respectively. We can further assume w.l.o.g. that each of a_1 and b_1 has at least one leg that lies between b_1 and b_2 , and between a_1 and a_2 , respectively. In fact, if one of these two vertices, say b_1 , does not have any such leg, then we may assume that the second fan-bundle is not anchored at b_1 but at a_2 , which is a case that has already been considered.

First, assume b_1 and b_2 are the only neighbors of a_1 that belong to some component of G . Then, either b_1 is a cutvertex or a_1 is the leftmost vertex on its layer that is not a leg of b_1 . In both cases, we move the legs of b_1 to the left of a_1 ; see Fig. 26a. Then, b_1 has no leg that lies between a_1 and a_2 , which contradicts our assumption.

Now, consider the case that b_1 and b_2 are not the only neighbors of a_1 that belong to some component of G . Assume first that a_1 and b_1 also belong to a $K_{2,3}$ component; see Fig. 26b. Assume w.l.o.g. that a_1 belongs to the partition set of the $K_{2,3}$ components containing the two vertices. We move the legs of a_1 that lie between b_1 and b_2 inside the $K_{2,3}$ component; see Fig. 26b. Then, as before, a_1 has no leg that lies between b_1 and b_2 , which contradicts our assumption. It remains to consider the case in which a_1 and b_1 belong to a second $K_{2,2}$ component; see Fig. 26c. Let a'_2 and b'_2 be the additional vertices of this $K_{2,2}$ component. If the only legs inside the second $K_{2,2}$ component, if any, are also attached only to a_1 and b_1 , then we can move all the legs attached to a_1 inside the first $K_{2,2}$ component and all the legs attached to b_1 inside the second $K_{2,2}$ component, which again contradicts our assumption; see Fig. 26c. It follows that the legs of the second $K_{2,2}$ component must be attached only to a'_2 and b'_2 .

By applying the above arguments for the second $K_{2,2}$ component, we either obtain a contradiction or we conclude that a'_2 and b'_2 belong to a third $K_{2,2}$ component with the same properties. By repeating the same argument, we will eventually obtain a chain of $K_{2,2}$ components, all with the same properties. At the end of this chain, there must be either a cutvertex, or a $K_{2,3}$ component, or the leftmost (or the rightmost) vertex of one of the two layers. Thus, one of the previous cases applies in order to derive a contradiction. This completes the proof that there is no leg between a_1 and a_2 , or between b_1 and b_2 .

To conclude the proof of the lemma, assume that there is a leg attached to a vertex of our $K_{2,2}$ component, say a_1 , that does not lie between b_1 and b_2 . Since there are legs neither between a_1 and a_2 nor between b_1 and b_2 , we can move this leg between b_1 and b_2 , which yields one of the cases that we have already considered before. \square

From the above discussion, it follows that a leg can only be attached to

- (i) the leftmost or rightmost vertex of a snake that is not a common cutvertex, if it belongs to a $K_{2,3}$ component, or
- (ii) a common cutvertex that belongs to two $K_{2,3}$ components, or

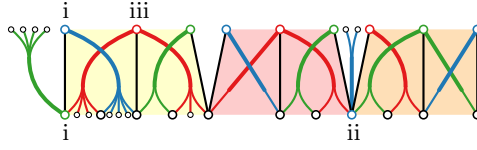


Figure 27: The baby stegosaurus from Fig. 23b with big legs. Each eligible vertex has at least one leg and the letters correspond to the cases that allow a leg to exist.

- (iii) a vertex that belongs to two $K_{2,3}$ components, and in each of them belongs to the partition set containing two vertices.

We refer to such a leg as *big leg*; see Fig. 27 for an example. This gives rise to the following simple recognition and drawing algorithm.

Theorem 24. *Maximal 1-sided 2-layer 1-fan-bundle-planar graphs can be recognized and drawn in linear time.*

Proof. We first remove all legs. By Lemma 22, the resulting graph has to be a baby stegosaurus. We split it at its cutvertices and use the recognition and drawing algorithm for snakes by Binucci et al. [7]. For each of the snakes, we can easily check whether it is a baby snake. In the negative case, we reject the instance. Otherwise, we glue the baby snakes together at their cutvertices. By Lemma 23, we only have to check whether the legs that we removed at the beginning of our algorithm are big legs, which can be done in linear time. In the negative case, we reject the instance. Otherwise, we draw each of them either between the two $K_{2,3}$ components it belongs to or at the leftmost or rightmost vertex on one of the layers, if this belongs to a $K_{2,3}$ component. \square

7.2 Triconnected 1-sided outer-1-fan-bundle-planar graphs.

In this section, we present a linear-time algorithm for the recognition of triconnected 1-sided outer-1-fbp graphs, which in the case of a positive instance also computes a corresponding 1-sided outer-1-fbp drawing. To do so, we will first present some important properties of triconnected 1-sided outer-1-fbp graphs. We start with a property of biconnected (and hence of triconnected) 1-sided outer-1-fbp graphs.

Lemma 25. *Let G be a biconnected 1-sided outer-1-fan-bundle-planar graph. A 1-sided outer-1-fan-bundle-planar drawing Γ of G can be augmented (by adding edges) into a 1-sided outer-1-fan-bundle-planar drawing Γ' in which all edges on the outer face of Γ' are planar.*

Proof. Let Π be the *planarization* of drawing Γ , i.e., Π is the drawing obtained by replacing the crossing points of Γ with dummy vertices. Since G is biconnected, the outer face of Π is a simple cycle and contains two types of vertices; vertices of G and vertices that correspond to crossing points of Γ . Let v_1, \dots, v_k be the vertices that are incident to the outer face of Π as they appear in clockwise order along it. Since Γ is outer-1-fbp, the outer face of Π contains all vertices of G .

Note that if the outer face of Π consists exclusively of vertices of G , then the lemma clearly holds. In particular, for any two vertices v_i and v_{i+1} of G that are consecutive along the outer face of Π , the edge (v_i, v_{i+1}) belongs to G ; see Fig. 28a. To complete the proof, assume that there exists a vertex, say v_i , along the outer face of Π that corresponds to a crossing point in Γ . By outer-1-fan-bundle-planarity, it follows that v_{i-1} and v_{i+1} are both vertices of G . We remove v_i from the outer face of Π as follows. If the edge (v_{i-1}, v_{i+1})



Figure 28: Creating an outer-1-fbp drawing in which all edges of its outer face are planar.

exists in G , we remove it from drawings Π and Γ . Then, we add the edge (v_{i-1}, v_{i+1}) to Π and to Γ as a curve that starts in v_{i-1} , follows the outer face until v_i , and ends in v_{i+1} again by following the outer face; see Fig. 28b.

Note that the aforementioned procedure does not reduce the number of vertices of G that are on the outer face of either Π or Γ , which implies that if we apply this procedure iteratively to each vertex of Π that corresponded to a crossing point of Γ , we will eventually obtain a drawing Γ' in which all edges of its outer face are planar. \square

Lemma 26. *The following properties hold in a 1-sided outer-1-fbp drawing Γ of a triconnected graph G in which all edges incident to its outer face are planar:*

P.1 No inner edge of Γ is planar.

P.2 The anchors of two crossing fan-bundles in Γ are consecutive along the outer face of Γ .

P.3 There is at most one fan-bundle crossing in Γ .

Proof. If there is an inner edge (u, v) that is planar in Γ , then u and v form a separation pair in G . Since G is triconnected, this is a contradiction. Hence, Property P.1 holds.

Let B_u and B_v be two crossing fan-bundles in Γ that are anchored at vertices u and v of G . To prove Property P.2, assume to the contrary that u and v are not consecutive along the outer face of Γ , i.e., (u, v) is not an edge of the outer face of Γ . We proceed by drawing edge (u, v) in Γ as a $B_u B_v$ -following curve (and hence planar), by first removing it from Γ in case that it belongs to G . Since u and v are not consecutive along the outer face of Γ , it follows that u and v form a separation pair in G . Since G is triconnected, this is a contradiction and Property P.2 holds.

To prove Property P.3, assume for a contradiction that there exist two fan-bundle crossings in Γ , say between fan-bundles B_u and B_v and between fan-bundles B_w and B_z , respectively. Clearly, $u \neq v$ and $w \neq z$ hold. Let u_1, \dots, u_κ and v_1, \dots, v_λ be the tips of B_u and B_v , respectively, in this clockwise order along the outer face of Γ . Accordingly, let w_1, \dots, w_μ and z_1, \dots, z_ν be the tips of B_w and B_z , respectively, in this clockwise order along the outer face of Γ . We now claim that $u \notin \{w, z\}$ and $v \notin \{w, z\}$ holds. Assume to the contrary that $v = w$. Then, by Property P.2, we may further assume w.l.o.g. that u, v and z appear consecutively in this clockwise order along the outer face of Γ ; see Fig. 29a. In this case, however, either $\langle v, z_\nu \rangle$ or $\langle v, u_1 \rangle$ form a separation pair in G , which is a contradiction to the fact that G is triconnected. So, we may assume that u, v, w and z are pairwise disjoint and w.l.o.g. that they appear in this clockwise order along the outerface of Γ ; see Fig. 29b. In this case, however, $\langle w, z_\nu \rangle$ or $\langle v, u_1 \rangle$ form a separation pair in G , which is again a contradiction to the fact that G is triconnected. Hence, Property P.3 holds. \square

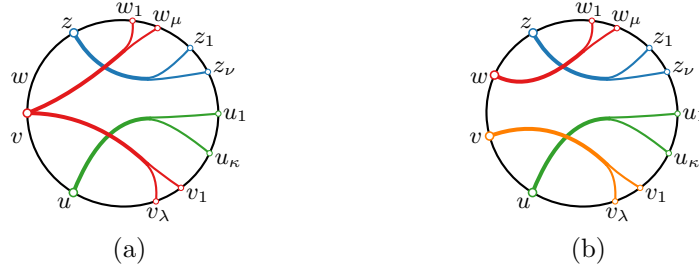


Figure 29: Illustration of the case of two fan-bundle crossings in Property P.3.

We call a drawing with Properties P.1, P.2 and P.3 of Lemma 26 a *canonical drawing*. In the following, we give a complete characterization of the triconnected 1-sided outer-1-fbp graphs.

Lemma 27. *A triconnected graph G with $n \geq 5$ vertices is 1-sided outer-1-fan-bundle-planar if and only if it consists of:*

- C.1 a Hamiltonian path v_1, v_2, \dots, v_n ,
- C.2 the edges (v_1, v_{n-1}) and (v_n, v_2) ,
- C.3 the edges (v_n, v_i) , with $3 \leq i \leq k-1$, and (v_1, v_j) , with $k \leq j \leq n-2$ for some $2 \leq k \leq n$,
- C.4 the edge (v_1, v_n) if $k \in \{2, n-1\}$, and
- C.5 possibly the edges (v_n, v_k) and (v_1, v_n) .

Proof. For the sufficiency part, in order to prove the triconnectivity, we show that there are at least 3 vertex-disjoint paths between each pair of vertices u and v of G . If $\{u, v\} = \{v_1, v_n\}$, then there exist paths v_1, v_2, v_n (by C.1 and C.2) and v_1, v_{n-1}, v_n (by C.3). For the third path, we choose the path v_1, v_k, v_{k-1}, v_n if $3 < k < n-1$ (which exists by C.3), the path v_1, v_{k+1}, v_k, v_n if $k = 3$ (which exists by $n \geq 5$), and the path v_1, v_n if $k \in \{2, n-1\}$ (which exists by C.4). Consider now a pair v_i and v_j of vertices, with $i < j$. Assume that $i < k$; the other case is symmetric. This implies that the edge (v_n, v_i) exists (by C.3). If $j < k$, then the edge (v_n, v_j) exists (by C.3) and v_i and v_j are connected by the path v_i, v_{i+1}, \dots, v_j , the path v_i, v_n, v_j , and the path $v_i, v_{i-1}, \dots, v_1, v_k, v_{k-1}, \dots, v_j$. If $j \geq k$, then the edge (v_1, v_j) exists (by C.3), and thus v_i and v_j are connected by the path v_i, v_{i+1}, \dots, v_j , the path $v_i, v_n, v_{n-1}, \dots, v_j$, and the path $v_i, v_{i-1}, \dots, v_1, v_j$. This proves the triconnectivity. Fig. 30 is an evidence that such a graph always admits a 1-sided outer-1-fbp drawing.

For the necessity, first assume that G is maximal 1-sided outer-1-fbp. By Lemma 25, there is a 1-sided outer-1-fbp drawing Γ whose outer face is a simple planar Hamiltonian cycle v_1, \dots, v_n, v_1 . Thus, C.1 holds. Since G is triconnected, there is at least one inner edge. By Lemma 26, Γ is canonical, and hence there exist exactly two crossing fan-bundles in Γ , whose origins v_n and v_1 are adjacent along the outer face of Γ . Since every vertex of G has degree at least 3, each vertex v_2, \dots, v_{n-1} is a tip of B_{v_n} or B_{v_1} . Also, since the edges belonging to B_{v_n} and B_{v_1} cannot be further crossed, it follows that the tips of B_{v_n} and of B_{v_1} form two interior-disjoint intervals along the outer face of Γ . Hence, all edges described by C.2 and C.3 belong to G ; the edges from C.2 have to exist since v_2 can only be a tip of B_{v_n} and since v_{n-1} can only be a tip of B_{v_1} by simplicity. Since G is maximal,

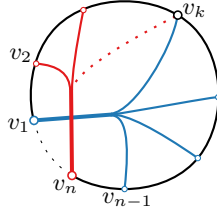


Figure 30: A 1-sided outer-1-fbp canonical drawing of a triconnected graph.

there exists a vertex v_k , with $2 \leq k \leq n - 1$, that is a tip of both B_{v_n} and B_{v_1} . Hence, C.4 and C.5 hold.

Assume now that G is not maximal. By Lemma 25, G is a subgraph of a maximal 1-sided outer-1-fbp graph G' . The only edges that can be removed from G' without violating triconnectivity are one of (v_1, v_k) and (v_n, v_k) , plus the edge (v_1, v_n) , but only if $k \notin \{2, n - 1\}$; otherwise, at least one of v_1 and v_n has degree smaller than 3. Hence, C.3, C.4 and C.5 hold. This also implies that the Hamiltonian cycle v_1, \dots, v_n, v_1 can become a Hamiltonian path v_1, \dots, v_n , and thus C.1 still holds. This concludes the proof of the lemma. \square

Based on Lemma 27, we can derive a linear-time recognition algorithm for triconnected graphs, which in the case of a positive instance also computes a 1-sided outer-1-fbp drawing. To this end, we have to find the Hamiltonian path v_1, \dots, v_n . While it is NP-hard in general to find a Hamiltonian path, we show that we can do so efficiently for this graph class by identifying the vertices v_1 and v_n based on their degree.

Theorem 28. *Triconnected 1-sided outer-1-fan-bundle-planar graphs can be recognized and drawn in linear time.*

Proof. Let G be any triconnected graph. The task is to test whether G satisfies the conditions C.1-C.5 of Lemma 27. Note that, in order for these conditions to be satisfied, the only vertices that can have degree larger than 3 are v_n , v_1 , and v_k . In particular, the sum of the degrees of v_1 and v_n is between n and $n + 3$, v_k has degree at most 4, while every other vertex has degree exactly 3. More specifically, the sum of the degrees of v_1 and v_n is

- n , if $\deg v_k = 3$ and edge (v_1, v_n) does not belong to G ;
- $n + 1$, if $\deg v_k = 4$ and edge (v_1, v_n) does not belong to G ;
- $n + 2$, if $\deg v_k = 3$ and edge (v_1, v_n) belongs to G ;
- $n + 3$, if $\deg v_k = 4$ and edge (v_1, v_n) belongs to G .

Hence, our algorithm rejects G if one of the following holds:

- there are more than three vertices with degree larger than 3;
- there are more than two vertices with degree larger than 4;
- there are no two vertices such that the sum of their degrees is between n and $n + 3$.

Fig. 31 shows all triconnected 1-sided outer-1-fbp graphs with $n \leq 8$. So, if G has at most eight vertices, our algorithm exhaustively tests whether G is one of these graphs. So, we may assume w.l.o.g. that G has at least nine vertices. Then, the sum of the degrees

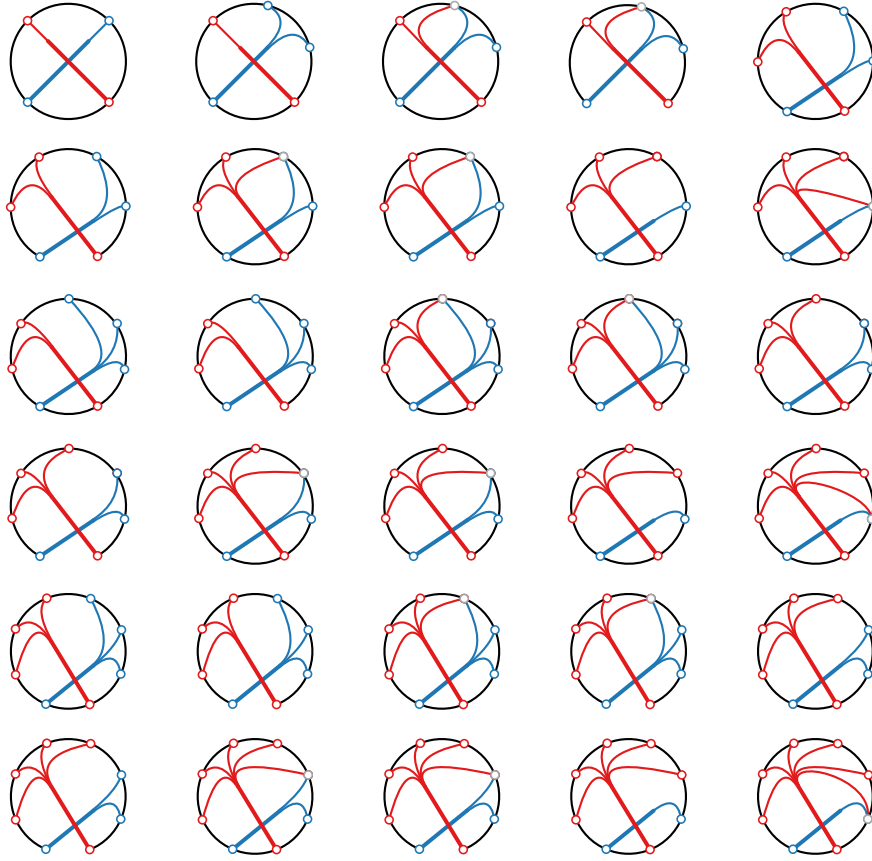


Figure 31: All triconnected 1-sided outer-1-fbp graphs with at most 8 vertices.

of v_1 and v_n must be at least 9, so there always exists at least one vertex of degree larger than 4. We distinguish the following cases. Table 2 gives an overview of the cases and shows that the case analysis is complete.

Case 1: *There are two vertices of G with degree larger than 4.* These two vertices must be v_1 and v_n . If we remove them from G , what remains must be a path v_2, \dots, v_{n-1} , which prescribes the Hamiltonian path together with (v_1, v_2) and (v_{n-1}, v_n) ; see Fig. 32a.

Case 2: *There is a vertex of G with degree at least $n - 3$, and every other vertex has degree 3.* We label the high-degree vertex as v_n , and we distinguish three subcases, based on its degree.

Case 2.1: $\deg(v_n) = n - 1$. Then, v_n is connected to all other vertices. Hence, if we remove v_n from G , what remains must be a cycle. So, we can choose any vertex as v_1 and one of its incident edges as B_{v_1} ; see Fig. 32b.

Case 2.2: $\deg(v_n) = n - 2$. Then, the sum of the degrees over all vertices of G is $n - 2 + 3 \cdot (n - 1) = 4n - 5$, which is not possible, since the sum of the degrees over all vertices of a graph is always even.

Case 2.3: $\deg(v_n) = n - 3$. Then, $\deg(v_1) + \deg(v_n) = n$, so the edge (v_1, v_n) does not exist. Hence, the three edges from v_1 are (v_1, v_2) , $(v_1, v_{n-2}) = (v_1, v_k)$, and (v_1, v_{n-1}) . Since $\deg(v_k) = 3$, the edge (v_k, v_n) does not exist, so v_n is connected to every vertex except for v_1 and v_k . We label as v_1 one of the two vertices that are not connected to v_n . If we now remove v_1 and v_n from G , what remains must be again a

Table 2: An illustration of all cases in the proof of Theorem 28 with $n \geq 9$ that can occur by $n \leq \deg v_n + \deg v_1 \leq n + 3$ and $3 \leq \deg v_k \leq 4$, assuming that $\deg v_n > 4 \geq \deg v_1$. The remaining case that $\deg v_n \geq \deg v_1 > 4$ is handled in Case 1. Columns marked by an X cannot occur because of $\deg v_n + \deg v_1 \geq n$.

	deg $v_1 = 4$		deg $v_1 = 3$	
	deg $v_k = 4$	deg $v_k = 3$	deg $v_k = 4$	deg $v_k = 3$
deg $v_n = n - 1$	Case 4	Case 3.1	Case 3.1	Case 2.1
deg $v_n = n - 2$	Case 4	Case 3.2.1	Case 3.2.2	Case 2.2
deg $v_n = n - 3$	Case 4	Case 3.1	Case 3.1	Case 2.3
deg $v_n = n - 4$	Case 4	Case 3.3	X	X

path v_2, \dots, v_{n-1} , which prescribes the Hamiltonian path together with (v_1, v_2) and (v_{n-1}, v_n) ; see Fig. 32c.

Case 3: *There is a vertex of G with degree at least $n - 4$, one vertex with degree 4, and each other vertex has degree 3.* We label the high-degree vertex as v_n , and we distinguish again three subcases.

Case 3.1: $\deg(v_n) = n - 1$ or $\deg(v_n) = n - 3$. In the former case, the sum of degrees over all vertices of G is $n - 1 + 4 + 3 \cdot (n - 2) = 4n - 3$, while in the latter case it is $4n - 5$; since in both cases this value is odd, we conclude that this case cannot occur.

Case 3.2: $\deg(v_n) = n - 2$. In this case, we do not know whether v_1 or v_k is the degree-4 vertex, so we have to try both possibilities.

Case 3.2.1: We label the degree-4 vertex as v_1 . Then, we have a similar situation as in Case 1, with the only difference being that the edge (v_k, v_n) does not exist. We thus proceed as in this case; see Fig. 32c.

Case 3.2.2: We label the degree-4 vertex as v_k . Then, v_1 has degree 3 and we have $\deg(v_1) + \deg(v_n) = n + 1$, so v_1 has to be the only vertex not adjacent to v_n . If we now remove v_n and v_1 from G , what remains must be again a path v_2, \dots, v_{n-1} , which prescribes the Hamiltonian path together with (v_1, v_2) and (v_{n-1}, v_n) ; see Fig. 32c.

Case 3.3: $\deg(v_n) = n - 4$. Since $\deg(v_1) + \deg(v_n) \geq n$, we have that v_1 must be the degree-4 vertex and the edge (v_1, v_n) does not exist. Then, since $\deg(v_k) = 3$, the edge (v_k, v_n) also does not exist. Hence, the situation is the same as in Case 1 (with these two edges missing); see Fig. 32a. Hence, we can again prescribe the Hamiltonian path by removing v_1 and v_n .

Case 4: *There is a vertex of G with degree at least $n - 4$, two vertices with degree 4, and every other vertex has degree 3.* We label the high-degree vertex as v_n . One of the vertices with degree 4 has to be v_1 , the other one has to be v_k . In any case, v_k will have degree 4, so both the edges (v_1, v_k) and (v_k, v_n) must exist. We distinguish two subcases based on whether one or both these degree-4 vertices are connected to v_n .

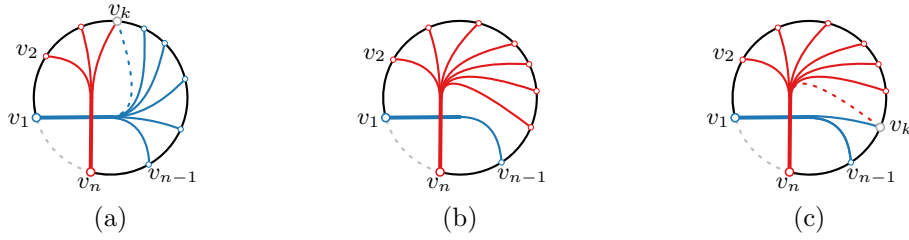


Figure 32: Illustration of the different cases for $n \geq 9$. Dotted edges might be there or not, depending on the case: (a) Cases 1, 3.3, and 4.1, (b) Case 2.1, and (c) Cases 2.3, 3.2, and 4.2

Case 4.1: One of the two degree-4 vertices is not connected to v_n . Since the edge (v_k, v_n) exists, this vertex must be v_1 . We can handle this case in the same way as Case 3.3; see Fig. 32a.

Case 4.2: Both degree-4 vertices are connected to v_n . In this case, the edge (v_1, v_n) exists. Since v_1 has degree 4, it has two inner edges: (v_1, v_{n-1}) and (v_1, v_{n-2}) with its other edges being (v_1, v_2) and (v_1, v_n) . This implies that $k = n - 2$, so v_k has edges (v_1, v_k) , (v_k, v_n) , (v_k, v_{n-1}) , and (v_k, v_{n-3}) ; thus v_1 and v_k only differ in one edge. In fact, by removing v_n and its incident edges we obtain a cycle with the single chord (v_1, v_k) , so the whole graph is symmetric and we can choose either of the degree-4 vertices as v_1 ; see Fig. 32c.

This completes the description of our recognition algorithm. We can find vertices v_1 and v_n and the Hamiltonian cycle in linear time and we can check whether the correct edges are in the graph in linear time as well, so the whole algorithm runs in linear time. In the case in which G is a positive instance, we obtain a 1-sided outer-1-fbp drawing as follows. If $n < 9$, then we directly construct the drawing as in Fig. 31. Otherwise, we identify the case of the proof and then create a drawing according to Fig. 32. \square

8 Conclusions

In this work, we studied a new drawing model, which introduces the visualization technique of edge-bundling in the framework of beyond-planarity, focusing in particular on the class of fan-planar graphs. Our work opens several research directions:

- Find recognition algorithms for 1- or 2-sided (biconnected) outer- or 2-layer 1-fbp graphs;
- close the gaps in the density bounds of Table 1;
- discuss relationships with other classes of nearly-planar graphs;
- study the k -fan-bundle-planarity, where each fan-bundle can be crossed at most k times;
- consider other models of edge bundling suitable for theoretical analyses and comparisons, e.g., allowing edges to be bundled together not only at their endpoints.

Acknowledgments

The authors would like to thank the anonymous reviewers for their constructive comments. This work is partially supported by the DFG grants Ka812/17-1 and Schu2458/4-1.

References

- [1] P. K. Agarwal, B. Aronov, J. Pach, R. Pollack, and M. Sharir. Quasi-planar graphs have a linear number of edges. *Combinatorica*, 17(1):1–9, 1997. doi:10.1007/BF01196127.
- [2] E. N. Argyriou, M. A. Bekos, and A. Symvonis. The straight-line RAC drawing problem is NP-hard. *J. Graph Algorithms Appl.*, 16(2):569–597, 2012. doi:10.7155/jgaa.00274.
- [3] C. Auer, C. Bachmaier, F. J. Brandenburg, A. Gleißner, K. Hanauer, D. Neuwirth, and J. Reislhuber. Outer 1-planar graphs. *Algorithmica*, 74(4):1293–1320, 2016. doi:10.1007/s00453-015-0002-1.
- [4] C. Auer, F. J. Brandenburg, A. Gleißner, and K. Hanauer. On sparse maximal 2-planar graphs. In W. Didimo and M. Patrignani, editors, *Proc. 20th Int. Symp. Graph Drawing (GD '12)*, volume 7704 of *LNCS*, pages 555–556. Springer, 2012. doi:10.1007/978-3-642-36763-2_50.
- [5] S. W. Bae, J.-F. Baffier, J. Chun, P. Eades, K. Eickmeyer, L. Grilli, S.-H. Hong, M. Korman, F. Montecchiani, I. Rutter, and C. D. Tóth. Gap-planar graphs. In F. Frati and K.-L. Ma, editors, *Proc. 25th Int. Symp. Graph Drawing (GD '17)*, volume 10692 of *LNCS*, pages 531–545. SV, 2017.
- [6] M. A. Bekos, S. Cornelsen, L. Grilli, S. Hong, and M. Kaufmann. On the recognition of fan-planar and maximal outer-fan-planar graphs. *Algorithmica*, 79(2):401–427, 2017. doi:10.1007/s00453-016-0200-5.
- [7] C. Binucci, M. Chimani, W. Didimo, M. Gronemann, K. Klein, J. Kratochvíl, F. Montecchiani, and I. G. Tollis. Algorithms and characterizations for 2-layer fan-planarity: From caterpillar to stegosaurus. *J. Graph Algorithms Appl.*, 21(1):81–102, 2017. doi:10.7155/jgaa.00398.
- [8] C. Binucci, E. Di Giacomo, W. Didimo, F. Montecchiani, M. Patrignani, A. Symvonis, and I. G. Tollis. Fan-planarity: Properties and complexity. *Theor. Comput. Sci.*, 589:76–86, 2015. doi:10.1016/j.tcs.2015.04.020.
- [9] R. Bodendiek, H. Schumacher, and K. Wagner. Über 1-optimale Graphen. *Math. Nachrichten*, 117(1):323–339, 1984. doi:10.1002/mana.3211170125.
- [10] F. J. Brandenburg. A simple quasi-planar drawing of K_{10} . In Y. Hu and M. Nöllenburg, editors, *Proc. 24th Int. Symp. Graph Drawing Netw. Vis. (GD '16)*, volume 9801 of *LNCS*, pages 603–604. Springer, 2016.
- [11] K. Buchin, B. Speckmann, and K. Verbeek. Flow map layout via spiral trees. *IEEE Trans. Vis. Comput. Graphics*, 17(12):2536–2544, 2011. doi:10.1109/TVCG.2011.202.

- [12] S. Chaplick and K. Verbeek. Geometric perspectives in graph drawing and information visualization. SoCG2017 Workshop, July 4th 2017.
- [13] O. Cheong, S. Har-Peled, H. Kim, and H. Kim. On the number of edges of fan-crossing free graphs. *Algorithmica*, 73(4):673–695, 2015. doi:10.1007/s00453-014-9935-z.
- [14] H. R. Dehkordi, P. Eades, S. Hong, and Q. H. Nguyen. Circular right-angle crossing drawings in linear time. *Theor. Comput. Sci.*, 639:26–41, 2016. doi:10.1016/j.tcs.2016.05.017.
- [15] E. Di Giacomo, W. Didimo, P. Eades, and G. Liotta. 2-layer right angle crossing drawings. *Algorithmica*, 68(4):954–997, 2014. doi:10.1007/s00453-012-9706-7.
- [16] E. Di Giacomo, W. Didimo, and G. Liotta. Spine and radial drawings. In R. Tamassia, editor, *Handbook on Graph Drawing and Visualization.*, pages 247–284. Chapman & Hall, 2013.
- [17] M. Dickerson, D. Eppstein, M. T. Goodrich, and J. Y. Meng. Confluent drawings: Visualizing non-planar diagrams in a planar way. In G. Liotta, editor, *Proc. 11th Int. Symp. Graph Drawing (GD '03)*, volume 2912 of *LNCS*, pages 1–12. Springer, 2003. doi:10.1007/978-3-540-24595-7_1.
- [18] W. Didimo, P. Eades, and G. Liotta. Drawing graphs with right angle crossings. *Theor. Comput. Sci.*, 412(39):5156–5166, 2011. doi:10.1016/j.tcs.2011.05.025.
- [19] P. Eades, S. Hong, N. Katoh, G. Liotta, P. Schweitzer, and Y. Suzuki. A linear time algorithm for testing maximal 1-planarity of graphs with a rotation system. *Theor. Comput. Sci.*, 513:65–76, 2013. doi:10.1016/j.tcs.2013.09.029.
- [20] R. B. Eggleton. Rectilinear drawings of graphs. *Utilitas Math.*, 29:149–172, 1986.
- [21] M. Fink, J. Hershberger, S. Suri, and K. Verbeek. Bundled crossings in embedded graphs. In E. Kranakis, G. Navarro, and E. Chávez, editors, *Proc. 12th Lat. Am. Symp. Theoret. Inform. (LATIN '16)*, volume 9644 of *LNCS*, pages 454–468. Springer, 2016. doi:10.1007/978-3-662-49529-2_34.
- [22] T. M. J. Fruchterman and E. M. Reingold. Graph drawing by force-directed placement. *Softw., Pract. Exper.*, 21(11):1129–1164, 1991. doi:10.1002/spe.4380211102.
- [23] M. Garey and D. S. Johnson. *Computers and Intractability: A Guide to the Theory of NP-Completeness*. W. H. Freeman & Co., New York, NY, USA, 1979.
- [24] M. Garey and D. S. Johnson. Crossing number is NP-complete. *SIAM J. Algebraic Discrete Methods*, 4(3):312–316, 1983. doi:10.1137/0604033.
- [25] D. Holten. Hierarchical edge bundles: Visualization of adjacency relations in hierarchical data. *IEEE Trans. Vis. Comput. Graphics*, 12(5):741–748, 2006. doi:10.1109/TVCG.2006.147.
- [26] D. Holten and J. J. van Wijk. Force-directed edge bundling for graph visualization. *Comput. Graph. Forum*, 28(3):983–990, 2009. doi:10.1111/j.1467-8659.2009.01450.x.
- [27] S. Hong, P. Eades, N. Katoh, G. Liotta, P. Schweitzer, and Y. Suzuki. A linear-time algorithm for testing outer-1-planarity. *Algorithmica*, 72(4):1033–1054, 2015. doi:10.1007/s00453-014-9890-8.

- [28] S. Hong and T. Tokuyama. Algorithmics for beyond planar graphs. NII Shonan Meeting Seminar 089, November 27 - December 1 2016.
- [29] M. Kaufmann, S. Kobourov, J. Pach, and S. Hong. Beyond planar graphs: Algorithmic and combinatorics. Dagstuhl Seminar 16452, November 6 - 11 2016.
- [30] M. Kaufmann and T. Ueckerdt. The density of fan-planar graphs. *ArXiv e-prints*, 1403.6184, 2014.
- [31] S. G. Kobourov, G. Liotta, and F. Montecchiani. An annotated bibliography on 1-planarity. *Computer Science Review*, 25:49–67, 2017. doi:<http://dx.doi.org/10.1016/j.cosrev.2017.06.002>.
- [32] J. Pach and G. Tóth. Graphs drawn with few crossings per edge. *Combinatorica*, 17(3):427–439, 1997. doi:[10.1007/BF01215922](https://doi.org/10.1007/BF01215922).
- [33] G. Ringel. Ein Sechsfarbenproblem auf der Kugel. *Abh. Math. Sem. Univ. Hamb.*, 29:107–117, 1965. doi:[10.1007/BF02996313](https://doi.org/10.1007/BF02996313).
- [34] K. Sugiyama, S. Tagawa, and M. Toda. Methods for visual understanding of hierarchical system structures. *IEEE Trans. Syst. Man Cybern.*, 11(2):109–125, 1981. doi:[10.1109/TSMC.1981.4308636](https://doi.org/10.1109/TSMC.1981.4308636).
- [35] A. Telea and O. Ersoy. Image-based edge bundles: Simplified visualization of large graphs. *Comput. Graph. Forum*, 29(3):843–852, 2010. doi:[10.1111/j.1467-8659.2009.01680.x](https://doi.org/10.1111/j.1467-8659.2009.01680.x).
- [36] H. Zhou, P. Xu, X. Yuan, and H. Qu. Edge bundling in information visualization. *Tsinghua Sci. Technol.*, 18(2):145–156, 2013.
- [37] H. Zhou, X. Yuan, H. Qu, W. Cui, and B. Chen. Visual clustering in parallel coordinates. *Comput. Graph. Forum*, 27(3):1047–1054, 2008. doi:[10.1111/j.1467-8659.2008.01241.x](https://doi.org/10.1111/j.1467-8659.2008.01241.x).